USACERL Technical Report FM-93/16
September 1993
New Technology for EMP/EMI Shielded Structures

US Army Corps
of Engineers
Construction Engineering
Research Laboratories

Electrochemical Behavior of Ion-plated TiN and Cu-Cr Coatings

by
Y.W. Lee
M. Metzger
J.M. Rigsbee

The electrochemical (corrosion) behaviors of titanium nitride (TiN) and metastable copper-chromium (Cu-Cr) alloy coatings grown on glass, aluminum, and copper substrates using a plasma-assisted physical vapor deposition (ion-plating) technique were investigated. Various polarization techniques were used for corrosion tests in oxygen-saturated and deaerated 5 percent Na_2SO_4 and 3.5 percent NaCl solutions of two different acidities (pH=6 and 3). The structure, chemistry, and morphology of the coating surfaces before and after corrosion testing were analyzed with scanning electron microscope, x-ray diffraction, Auger, and x-ray photoelectron spectroscopic techniques.

Titanium nitride coatings are chemically passive but do not provide effective protection for metallic substrates, under conditions involving pitting corrosion, due to the presence of "pinholes" in the as-deposited TiN coatings. The inherent properties of TiN do appear suitable for electromagnetic interference/electromagnetic pulse shield applications provided the problem of film defects (porosity, pinholes) can be solved or if the substrate type and corrosion conditions are such that passivation of the substrate surface occurs. Cu-Cr alloy coatings show a general corrosion behavior, with corrosion rates of a few mils per year at the free corrosion potential, which is unsatisfactory for a thin film coating application.

The contents of this report are not to be used for advertising, publication, or promotional purposes. Citation of trade names does not constitute an official endorsement or approval of the use of such commercial products. The findings of this report are not to be construed as an official Department of the Army position, unless so designated by other authorized documents.

DESTROY THIS REPORT WHEN IT IS NO LONGER NEEDED

DO NOT RETURN IT TO THE ORIGINATOR

USER EVALUATION OF REPORT

REFERENCE: USACERL Technical Report (TR) FM-93/16, *Electrochemical Behavior of Ion-plated TiN and Cu-Cr Coatings*

Please take a few minutes to answer the questions below, tear out this sheet, and return it to USACERL. As user of this report, your customer comments will provide USACERL with information essential for improving future reports.

1. Does this report satisfy a need? (Comment on purpose, related project, or other area of interest for which report will be used.)

_____

_____

_____

2. How, specifically, is the report being used? (Information source, design data or procedure, management procedure, source of ideas, etc.)

_____

_____

3. Has the information in this report led to any quantitative savings as far as manhours/contract dollars saved, operating costs avoided, efficiencies achieved, etc.? If so, please elaborate.

_____

_____

4. What is your evaluation of this report in the following areas?

   a. Presentation:_____

   b. Completeness:_____

   c. Easy to Understand:_____

   d. Easy to Implement:_____

   e. Adequate Reference Material:_____

   f. Relates to Area of Interest:_____

   g. Did the report meet your expectations?_____

   h. Does the report raise unanswered questions?_____

i. General Comments. (Indicate what you think should be changed to make this report and future reports of this type more responsive to your needs, more usable, improve readability, etc.)

_____

_____

_____

_____

_____

5. If you would like to be contacted by the personnel who prepared this report to raise specific questions or discuss the topic, please fill in the following information.

Name: _____

Telephone Number: _____

Organization Address: _____

_____

_____

6. Please mail the completed form to:

Department of the Army
CONSTRUCTION ENGINEERING RESEARCH LABORATORIES
ATTN: CECER-IMT
P.O. Box 9005
Champaign, IL 61826-9005

REPORT DOCUMENTATION PAGE

Form Approved
OMB No. 0704-0188

1. AGENCY USE ONLY (Leave Blank)	2. REPORT DATE	3. REPORT TYPE AND DATES COVERED
	September 1993	Final

4. TITLE AND SUBTITLE
Electrochemical Behavior of Ion-plated TiN and Cu-Cr Coatings

5. FUNDING NUMBERS
4A162784
AT41
B-036

6. AUTHOR(S)
Y.W. Lee, M. Metzger, and J.M. Rigsbee

7. PERFORMING ORGANIZATION NAME(S) AND ADDRESS(ES)
U.S. Army Construction Engineering Research Laboratories (USACERL)
P.O. Box 9005
Champaign, IL 61826-9005

8. PERFORMING ORGANIZATION REPORT NUMBER
TR-FM-93/16

9. SPONSORING/MONITORING AGENCY NAME(S) AND ADDRESS(ES)
Headquarters, U.S. Army Corps of Engineers (HQUSACE)
ATTN: CEMP-EE
20 Massachusetts Avenue, NW.
Washington, DC 20314-1000

10. SPONSORING/MONITORING AGENCY REPORT NUMBER

11. SUPPLEMENTARY NOTES
Copies are available from the National Technical Information Service, 5285 Port Royal Road, Springfield, VA 22161

12a. DISTRIBUTION/AVAILABILITY STATEMENT
Approved for public release; distribution is unlimited.

12b. DISTRIBUTION CODE

13. ABSTRACT (Maximum 200 words)

The electrochemical (corrosion) behaviors of titanium nitride (TiN) and metastable copper-chromium (Cu-Cr) alloy coatings grown on glass, aluminum, and copper substrates using a plasma-assisted physical vapor deposition (ion-plating) technique were investigated. Various polarization techniques were used for corrosion tests in oxygen-saturated and deaerated 5 percent Na_2SO_4 and 3.5 percent NaCl solutions of two different acidities (pH=6 and 3). The structure, chemistry, and morphology of the coating surfaces before and after corrosion testing were analyzed with scanning electron microscope, x-ray diffraction, Auger, and x-ray photo-electron spectroscopic techniques.

Titanium nitride coatings are chemically passive but do not provide effective protection for metallic substrates, under conditions involving pitting corrosion, due to the presence of "pinholes" in the as-deposited TiN coatings. The inherent properties of TiN do appear suitable for electromagnetic interference/electromagnetic pulse shield applications provided the problem of film defects (porosity, pinholes) can be solved or if the substrate type and corrosion conditions are such that passivation of the substrate surface occurs. Cu-Cr alloy coatings show a general corrosion behavior, with corrosion rates of a few mils per year at the free corrosion potential, which is unsatisfactory for a thin film coating application.

14. SUBJECT TERMS
electromagnetic shielding
coatings
TiN coatings
Cu-Cr coatings
corrosion resistance

15. NUMBER OF PAGES
40

16. PRICE CODE

17. SECURITY CLASSIFICATION OF REPORT	18. SECURITY CLASSIFICATION OF THIS PAGE	19. SECURITY CLASSIFICATION OF ABSTRACT	20. LIMITATION OF ABSTRACT
Unclassified	Unclassified	Unclassified	SAR

FOREWORD

This investigation was performed for Headquarters, U.S. Army Corps of Engineers (HQUSACE) under Project 4A162731AT41, "Military Facilities Engineering Technology"; Task Area B, "Construction Management Technology"; Work Unit 036, "New Technology for EMP/EMI Shielded Structures." The HQUSACE technical monitor was L. Horvath (CEMP-EE).

This investigation was performed for the Engineering and Materials Division (FM) of the Infrastructure Laboratory (FL), U.S. Army Construction Engineering Research Laboratories (USACERL) by Dr. Y. W. Lee, Professor J.M. Rigsbee, and the late Professor M. Metzger of the Department of Materials Science and Engineering, University of Illinois, Urbana, IL. Dr. W.J. Croisant was the USACERL principal investigator. Vincent Hock directed the ion-plating facility at USACERL. The authors are grateful to J. Givens for preparing TiN coatings and to the staff of the Materials Research Laboratory at the University of Illinois for their assistance with the chemical analysis. USACERL's Electromagnetic Pulse Team Leader was Ray G. McCormack. Dr. Paul Howdyshell is Chief, CECER-FM. Dr. Michael J. O'Connor is Chief, CECER-FL. The USACERL technical editor was Gloria J. Wienke, Information Management Office.

LTC David J. Rehbein is Commander of USACERL and Dr. L.R. Shaffer is Director.

CONTENTS

FIGURES

FIGURES (cont'd)

ELECTROCHEMICAL BEHAVIOR OF ION-PLATED TiN AND Cu-Cr COATINGS

1 INTRODUCTION

Background

The Army is concerned about protecting electronic equipment from electromagnetic interference (EMI), including electromagnetic pulse (EMP). Equipment susceptible to EMI is placed within electromagnetically shielded enclosures. One cause of degradation of the shielding effectiveness of electromagnetically shielded enclosures is gasket failure, particularly around doors. To improve the performance of the shelters, it is essential to minimize this degradation. One technique to improve shielding effectiveness is to apply a hard, durable, and electrically conductive coating on the interfaces of gaskets and seals.

Thin layer metallic or ceramic coatings have been widely used on structural materials for a variety of applications such as wear and corrosion resistance. For example, titanium nitride (TiN) is commercially used as a hardfacing coating to prolong the life of cutting tools and as a decorative coating on such items as watches where corrosion resistance is required.

New uses of coatings have been continuously emerging to meet technological needs. One example being considered in this study is to use the electrically conductive property of the thin film as a protective coating for gaskets and seals for electromagnetic interference (EMI) mitigation. This report describes an effort to find a suitable coating material for the EMI shield application.

The shielding effectiveness of a coating depends on many factors such as the electrical conductivity. The long term performance depends on the mechanical and chemical properties of the coating materials as well as adhesion between the coating and substrate. Good bulk electrical conductivity and low contact resistance of the coating are of prime importance for this application. The coating must be hard and strong to minimize wear during service. It must also be chemically stable to resist environmental attack and be capable of protecting the substrate from corrosion in order to maintain effective shielding. In this study, two coating materials were initially considered candidates for EMI shielding: TiN and copper-chromium (Cu-Cr) alloy coatings fabricated via a plasma-assisted physical vapor deposition (ion-plating) technique.

TiN is a well known and widely used coating material that has industrial applications ranging from tribological (Ramalingan and Winer 1980; Jamal, Nimmagadda, and Bunshah 1980) to protective (Zeger, Kornman, and Aniquet 1977) and decorative (Wittmer 1985) coatings. TiN is hard and strong and has a thermal expansion coefficient of 9.35×10^{-6} per degree Kelvin (/K) at room temperature (Hintermann 1981). The most attractive property of TiN for shielding is its good electrical conductivity. The electrical resistivity of coated TiN on glass is approximately 100 micro-ohm-centimeters ($\mu\Omega$-cm) (N. Sicilian and W. Croisant, U.S. Army Construction Engineering Research Laboratories [USACERL], personal communication) which is substantially greater than that of both copper and aluminum but is comparable to that of many other metallic conductors.

Metastable single phase Cu-Cr alloys rich in copper are relatively new coating materials (Shin et al. 1983; Kim and Yee 1985), hence the properties of these materials are virtually unknown. It is, however, suggested that metastable Cu-Cr coatings may possess adequate electrical conductivity, corrosion resistance, and reasonable hardness suitable for the EMI shield application.

Considering only electrical and mechanical properties, both TiN and Cu-Cr alloy coatings should be suitable coating materials for the application. However, the corrosion properties of these coatings and the protectiveness of these coatings for the metallic substrates are not available in published literature.

Objective

The primary objective of this work was to examine and analyze the electrochemical (corrosion) behavior of ion-plated TiN and metastable Cu-Cr alloy coatings for possible application to EMI/EMP shielding. The sample coatings were fabricated at the ion-plating facility at the U.S. Army Construction Engineering Research Laboratories (USACERL). Commercial TiN coatings were evaluated to provide information for comparison.

Approach

The study was conducted in two parts. The first part characterized the degree of corrosion resistance of the coating materials. Coatings on glass substrates were used for this purpose. The second part characterized the corrosion behavior of TiN and Cu-Cr coatings on metallic (copper and aluminum) substrates to evaluate the protection effectiveness of the coating for metallic substrates.

Mode of Technology Transfer

It is recommended that a summary of information gained from this study be incorporated in Technical Manual (TM) 5-855-5, *Nuclear Electromagnetic Pulse (NEMP) Protection* (Department of the Army, February 1974) and Engineer Pamphlet (EP) 1110-3-2, *Electromagnetic Pulse (EMP) and TEMPEST Protection for Facilities* (Headquarters, U.S. Army Corps of Engineers, 31 December 1990).

2 EXPERIMENTAL METHODS

Commercially available microscopic glass slides, CDA 110 Cu, 1100 Al, and 6061-T6 Al were used as substrates. Substrate disks 0.625-in. (1.6-cm) diameter were prepared so that the coated disks could be inserted directly into the specimen holder of the electrochemical cell. Cu and Al substrates were ground and mechanically polished. Before coating, the substrates were cleaned in acetone and methanol (10 minutes each) using ultrasonic agitation.

Deionized water (electrical resistivity of 1 to 2 mega-ohm-centimeters [MΩ-cm]) and reagent grade sodium chloride (NaCl) and sodium sulfate (Na_2SO_4) were used to prepare the chloride and sulfate solutions. These solutions were chosen to simulate service environments of industrial and seacoast locations. Hydrogen chloride (HCl) was added to chloride solutions and sulphuric acid (H_2SO_4) was added to Na_2SO_4 solutions for acidity adjustments. Oxygen saturated solutions were prepared by passing high purity oxygen gas (O_2) into the electrolytes for 30 minutes. Deaerated solutions were made by passing pure nitrogen gas (N_2) into the electrolytes for at least 12 hours. These gases were continuously supplied during the corrosion tests and, as a consequence, the electrolytes were moderately agitated during the tests.

The electrochemical cell, with a capacity of 1000 cm^3 (61 cu in.), consists of a specimen holder, counter electrode (two graphite rods), reference electrode (saturated calomel electrode), and gas inlet and outlet leads. The specimen holder exposes a testing area of 1 cm^2 (0.155 sq in.) while maintaining sealing and electrical contact.

Several types of short term electrochemical testing techniques were used: linear polarization technique to estimate a corrosion rate, potentiodynamic polarization technique for a general understanding of corrosion behavior, and potentiostatic polarization technique to control the exact amount of current passing through the corrosion sample. Scanning rates were 0.1 and 0.2 millivolts per second (mV/s) for linear and potentiodynamic polarization tests, respectively. After the corrosion tests, samples were broken into several sections for structure and chemistry analysis. Scanning electron microscope (SEM), x-ray diffraction, Auger electron, and x-ray photoelectron spectroscopic techniques were used for the analysis. Wavelength dispersive x-ray analyses were used to determine the chemistry of Cu-Cr coatings.

3 RESULTS AND DISCUSSION

TiN Coatings

As-deposited TiN coatings, fabricated at USACERL using the ion-plating technique, were evaluated in terms of coating morphology, chemistry, and crystal structure. A few commercially fabricated TiN coatings were also studied for comparison. A visible difference between the commercial and USACERL TiN coatings is their color. TiN coatings fabricated at USACERL typically exhibit a brownish yellow color and commercially fabricated TiN coatings show a gold color.

In spite of the color difference, these two coatings were determined to be stoichiometric TiN based on the x-ray diffraction (XRD) spectra. XRD from a USACERL TiN coating on a glass substrate (Figure 1, curve A*) shows several peaks of stoichiometric TiN and a small peak of hexagonal Ti, indicating that USACERL TiN is stoichiometric but contains a small amount of Ti. On the other hand, only diffraction peaks pertaining to stoichiometric TiN are observed in the commercially fabricated TiN coating on a glass substrate (Figure 1, curve B). It is worthwhile to note that the structure of the USACERL TiN has a (200) preferred orientation while the structure of the commercial TiN has a (111) preferred orientation.

For microchemistry analysis, both TiN coatings were examined with x-ray photoelectron spectroscopy (XPS). Pure Ti was also included for reference purposes. Figure 2 shows XPS spectra of Ti $2p_{3/2}$ and $2p_{1/2}$ binding energies from pure Ti (curve A), commercial TiN (curve B), and from USACERL TiN (curve C). Before the acquisition of these spectra, about 10 to 20 angstroms (Å) of the surface was removed by argon- (Ar) ion bombardment. Note that $2p_{3/2}$ binding energy at 454 electronvolts (eV) from pure Ti is shifted to 455.4 eV for both TiN coatings. Also, for both coatings, very small peaks at 458 eV appear as "shoulders" on the larger peaks at 455.4 eV. These peaks (at different binding energy values) indicate different chemical environments for Ti which result in a shift in electron binding energy. By comparing with the published binding energy values of Ti 2p (Robinson and Sherwood 1984; Meletis, Carter, and Hochman 1984), the peak at 454 eV is identified as elemental Ti, the peak at 455.4 eV is Ti in the form of stoichiometric TiN and the peak at 458 eV is Ti in the form of TiO_2. The spectra of B and C in Figure 2 show that both coatings are stochiometric TiN but also contain small amount of TiO_2 in surface layers. Comparison of peak heights at 458 eV indicates that commercial TiN contains much more TiO_2 than USACERL TiN.

To examine the microchemistry of subsurface TiN coatings, about 100 Å of coating was removed by sputtering. Resulting XPS spectra are shown in Figure 3; spectra B-a for commercial TiN and C-a for USACERL TiN. The spectrum in Figure 2 were also included (as B and C) in Figure 3 to compare the surface and subsurface chemistries. Note that the peak height for TiO_2 (at 458 eV) for commercial TiN at the very surface layer (spectrum B) is substantially reduced in the same sample for the subsurface layer (spectrum B-a). This indicates that a small amount of TiO_2 may be present throughout the commercial TiN. On the other hand, XPS for the USACERL TiN coating after removing 100 Å (spectrum C-a) exhibits virtually no TiO_2, suggesting that $Ti)_2$ is present only near the surface of the USACERL TiN.

It is emphasized that the elemental Ti peak is absent in the XPS spectra for the USACERL TiN in Figure 3. This contradicts the XRD result (Figure 1) that detected elemental Ti for the same sample. XPS should detect elemental Ti observed by XRD, considering the similar sensitivity factors of the techniques. A possible explanation for this contradiction is that all (or a majority of) elemental Ti detected by XRD may be present near the interface between the glass substrate and TiN coating rather than as a random

*Figures are located at the end of the text, starting on p 19.

dispersion throughout the TiN. The escape depth of photoelectrons is at most a few nanometers and that of a diffracted x-ray beam is a few micrometers, indicating that surface analysis by XPS should not detect Ti if the Ti mainly exists as an interface layer. Because this is only a hypothesis to explain the contradictive experimental observations, more extensive study (such as transmission electron microscopy [TEM]) is needed to prove the hypothesis, since elemental Ti in TiN may seriously affect the electrochemical behavior of TiN coatings.

Nitrogen 1s (N1s) binding energies were also evaluated and their spectra are shown in Figure 4 (A for commercial TiN and B for USACERL TiN at about 100 Å subsurfaces). The main peak at about 397 eV is identified as nitrogen from stoichiometric TiN. The small peak at approximately 399.7 eV is, with some reservation, assigned to nitrogen of titanium oxy-nitride (TiO_xN_y) following work by Robinson and Sherwood (1984). Comparison of the two spectra indicates that commercial TiN contains more TiO_xN_y than USACERL TiN.

It is worthwhile to note that Ti $2p_{3/2}$ binding energy from TiO_xN_y is somewhat between Ti binding energies from TiN and from TiO_2, depending on the exact chemistry of TiO_xN_y (Robinson and Sherwood 1984). It is possible that the Ti $2p_{3/2}$ peaks in Figure 3 may consist of three peaks from TiN, TiO_2 and TiO_xN_y, which will be more consistent with the N1s spectra in Figure 4.

Experimental evidence thus far has shown a notable difference in microchemistry between the two TiN coatings. Commercial TiN, which exhibits a gold color, contains more TiO_2 and TiO_xN_y than the USACERL TiN which does not show a "gold" color. The origin of the color difference has not been identified. It could be very informative to compare electrochemical behavior of these two coatings. However, as only a few commercial TiN coatings on glass substrates were available, corrosion testing of commercial TiN is very limited in this study.*

Figure 5 is a SEM micrograph of as-deposited TiN coating surface on Al substrate which shows typical surface morphology with a columnar structure. Similar coatings at low magnifications are shown in Figure 6-A for TiN on a glass substrate and in Figure 6-B for TiN on an Al substrate. A number of small pores of a few micrometers in size are clearly visible in the TiN coating on Al, while they are not visible in the coating on glass. Submicroscopic pores, however, were observed in the TiN coating on glass. Auger analysis of TiN coating (Figure 7), shows only Ti and N peaks, suggesting that the coating is practically free of impurities.

Corrosion Testing of TiN on Glass

The basic corrosion tests were relatively rapid potentiodynamic scans and potentiostatic measurements of current density versus time. The main points of interest are: one, whether the coating itself shows low anodic current which is characteristic of passive behavior; and two, whether the coating deposited on metallic substrate protects the substrate. These points are discussed below.

Anodic and cathodic polarization scans for TiN coatings on glass substrates in 3.5 percent NaCl, pH=6.0, are shown in Figure 8 (A in oxygen saturated solutions and B in deaerated solutions). In both cases, the TiN coatings show an anodic current density of a few microamperes per square centimeter ($\mu A/cm^2$) up to +300 mV versus SCE (saturated calomel electrode), indicative of a passive behavior in this potential range. The anodic current density increases to approximately 10 $\mu A/cm^2$ at about 600 mV versus SCE. Considering the well known chemical stability of TiN, an anodic current density of a few to about 10 $\mu A/cm^2$ is higher than expected. A current density of a few microamperes per square centimeter is

*TiN coatings, if not otherwise noted in this report, imply coatings fabricated at USACERL.

approximately equivalent to a few mils per year of corrosion rate (Fontana and Green 1986). The usual rule that a few mils per year of corrosion rate is satisfactory as a "low" corrosion rate for engineering materials does not apply to a thin coating that is only a few micrometers thick. In spite of a relatively high current density, the TiN coatings appear to the unaided eye unchanged by the anodic polarization tests. SEM micrographs also show no evidence of coating corrosion. These apparently conflicting results do not explain satisfactorily the corrosion resistance of the coatings but raise an important question: What is the origin of the relatively high anodic current that does not cause morphological change on the TiN coating surface?

To answer this question, a commercial TiN on glass substrate was potentiodynamically scanned in the same solution, (Figure 8, Curve C). Note that the commercial TiN shows an anodic current of about 0.1 $\mu A/cm^2$ which is about 50 times lower than that of USACERL TiN. SEM examinations of the corrosion tested sample show no apparent corrosion as in the case of USACERL TiN.

The significant difference in anodic current density between the two sets of TiN coatings may be explained in terms of microchemistry differences. Earlier, it was discussed that a small amount of Ti may be concentrated at the interface between the glass substrate and the USACERL TiN coating. During the polarization test, Ti may easily be dissolved through pores (or pinholes), causing the increase in anodic current. The surface morphology of TiN coating should not be changed because the electrochemical reaction occurs mainly at the interface.

The USACERL TiN was potentiostatically polarized to study surface chemistry changes under controlled amounts of anodic current. The testing solution was 3.5 percent NaCl, pH=6.0. Polarization curves are given in Figure 9. The dashed lines indicate data for the deaerated solution and the solid lines indicate data for the oxygen saturated solution. Current densities are indicated by "i" and coulombs by "C," which is simply:

$$C = \int_0^t i \, dt$$

where t is time in seconds. Both samples were polarized at +300 mV versus SCE to 0.003 C/cm^2. Note that "i" in the deaerated solution is initially high and decreases rather rapidly with time while "i" in the oxygen saturated solution is low and decreases slowly with time. Accordingly, "C" increases more rapidly in a deaerated solution than in an oxygen saturated solution.

Figure 10 shows XPS spectra of Ti $2p_{3/2}$ and $2p_{1/2}$ binding energies from the potentiostatically tested TiN coatings of Figure 9. Spectra A and B are from about 10 and 100 Å from the surface after the test in an oxygen saturated solution and spectra C and D are from about 10 and 100 Å from the surface after the test in a deaerated solution. If the spectra A and C in Figure 10 are compared with the spectrum C in Figure 3, one could easily note by the peak height change at 458 eV that the amount of TiO_2 at the surface of TiN is increased after the test in oxygen saturated solution, and it is diminished after the test in deaerated solution. Spectra B and D indicate the absence of TiO_2 at a 100 Å depth from the surface, suggesting that chemistry changes during the corrosion tests are confined to a few atomic surface layers. The increased amount of TiO_2 during the corrosion test in an oxygen saturated solution may be responsible for the lower current density observed during the test shown in Figure 9.

It is not quite understood why TiN coating in a deaerated solution behaves differently from that in an oxygen saturated solution at the same potential. In principle, an anodically polarized sample in a deaerated solution should show the same results as that in an oxygen saturated solution. The difference may be explained by the difference in experimental conditions. Before the polarization tests, the TiN

coating was exposed to the testing solutions for some time until the steady state corrosion potentials were reached. In an oxygen saturated solution, the time to reach steady state corrosion potential is about 10 minutes, but it is usually more than 1 hour in a deaerated solution. Because of this significant time difference, the working electrode (TiN coating) in the oxygen saturated solution may have been in a very different electrochemical state from the one in the deaerated solution when polarization tests began, possibly resulting in different polarization curves (Figure 9) and different surface chemistry (Figure 10).

It is emphasized that the elemental form of Ti is not detected in the spectrum of corrosion tested samples (Figure 10). This is consistent with the spectrum of USACERL TiN and with the earlier discussion that the high anodic current of the USACERL TiN may be caused by the dissolution of elemental Ti present possibly at the interface. During polarization tests, Ti will be transported through pores or pinholes. Thus, the XPS technique should not detect the elemental form of Ti in the corrosion tested samples.

XPS spectra of nitrogen 1s for the same samples are compared with the spectra for an as-deposited sample in Figure 11. A small peak at approximately 399.7 eV, assigned to TiO_xN_y, in the as-deposited sample (spectrum A) is reduced by the corrosion test in an oxygen saturated solution (spectrum B) and it entirely disappears in a deaerated solution (spectrum C). This may suggest that TiO_xN_y is not a stable compound and it dissociates under the corrosive environment. Thermodynamic data of TiO_xN_y are not available, hence it is not possible to test the stability of this compound. Total absence of TiO_xN_y in spectrum C may be partially explained by the higher current density in this sample (observed in Figure 9).

Based on these results, TiN coating itself is basically passive and deterioration of the coating quality is not observed during short-term corrosion tests, indicating the high chemical stability of TiN. However, the increased amount of TiO_2 after the short-term test, evidenced by the XPS analysis, may cause a problem during a long-term service life. TiO_2 is an insulator and the formation of an insulating layer on the surface of TiN may increase contact resistance. It is suggested that a study be conducted to determine how contact resistance changes due to the formation of TiO_2 affect the EMI shielding effectiveness.

Corrosion Testing of TiN/Al and TiN/Cu

CDA 100 Cu, 1100 Al, and 6061-T6 Al alloy substrates and ion-plated TiN coatings on these substrates were potentiodynamically scanned in oxygen saturated 3.5 percent NaCl, pH=3.0 (Figure 12). Note that the polarization curve of TiN/Cu follows the same general shape as the pure Cu but at a lower current. This is, however, still much higher than that of TiN/glass. A different situation prevails with TiN/Al which shows almost the same polarization curve as does the 1100 Al substrate. The corrosion potential of TiN/Al is close to that of Al, and it is about 0.9 V below that of TiN/glass. Similar polarization curves were obtained when the acidity of the solution was decreased to pH=6.0 (Figure 13). The main difference between the data represented in Figures 12 and 13 is that in pH=6.0 solution, the polarization curve of TiN/Cu is closer to that of TiN/glass. It is also clear from Figures 12 and 13 that in a NaCl solution the TiN coating protects the Cu substrate to some degree, but it does not protect the Al substrate. As explained below, this may be due to the different electrochemical behavior of Cu and Al (pitting of Al and general corrosion of Cu in a NaCl solution).

Figure 14-A shows that a cluster of pits formed in TiN/Al has spread under the TiN coating and broken the TiN coating (Figure 14-B). SEM micrographs of cross sections through pits are shown in Figure 15 (A at 100 X magnification and B at 2000 X magnification) at the edge of the pit. Figure 15-B clearly shows cracking and spalling of the undercut TiN coating, but no visible corrosion of the TiN itself. Even though pitting of Al in a chloride solution is a well known phenomenon (de De Micheli 1978; Rais, Dalard, and Sohn 1985), a question arises as to how the pitting of Al substrates nucleates and grows under the TiN coating.

The basic problem is the "pinholes" in the TiN coating applied to Al as shown in Figure 6-B. Because of the number of pinholes, the TiN/Al specimen is essentially a bielectrode with a major fraction of its area composed of TiN and a minor fraction composed of Al as schematically shown in Figure 16-A. When the specimen is immersed in an NaCl solution, the pit may nucleate at the surface of the exposed Al. The current density for pitting corrosion on such a small area of exposed Al is so high that this small area dominates the electrochemical behavior of TiN/Al, resulting in a TiN/Al polarization curve very similar to that of bulk Al as shown in Figures 12 and 13. As the pit enlarges, it undercuts the TiN coating (Figure 16-B) and finally causes cracking and spalling of the TiN coating as schematically shown in Figure 16-C. It is, however, emphasized that nucleation of pits on the exposed Al of TiN/Al has not been directly observed because the pits spread so fast.

Due to general corrosion and the low corrosion rate of Cu in an NaCl solution,* TiN coating on Cu reduces the anodic current of Cu by reducing the Cu area exposed to the testing solution. Hence, TiN coatings improve the corrosion resistance of Cu in an NaCl solution. SEM examination of these samples does not show significant changes in the TiN coatings. The corrosion resistance may be further improved when an aerated solution, rather than an oxygen saturated solution, is used because, in an aerated solution, the free corrosion potential will be lowered, giving a somewhat reduced corrosion rate.

The bielectrode nature of TiN/Al due to pinholes in the TiN coating may cause a serious engineering problem due to galvanic effects. In a TiN/Al system, TiN is a cathode and exposed Al is an anode. Because of the large difference in the exposed area, the area ratio of cathode over anode could be 100 or more depending on the size and density of the pinholes. The high current density observed in Figures 12 and 13 is essentially concentrated on the small Al area, causing fast pit growth. For bulk Al, the area ratio of cathode over anode should be much smaller than that for TiN/Al, resulting in a wide spread of the anodic current and a reduction in the local anodic current density. The wide spread of anodic current on bulk Al will cause more nucleation of pits and the reduced local current density will slow the pit growth rate. The example of this discussion is in Figure 17 which shows a wide spread of small pits (about 10μm in size) on the bulk Al surface after an anodic polarization test in 3.5 percent NaCl, pH=6.0. These pits are much smaller than those on TiN/Al which are several hundred micrometers (previously shown in Figure 14-A). The larger and deeper pits of TiN/Al are due to an enhanced galvanic reaction which is not desirable for structural component applications.

TiN on 6061-T6 Al alloy behaves very similar to the TiN/Al but at a slightly lower current as shown in Figure 18. SEM micrographs of this system are essentially the same as Figures 14, 15, and 17.

The electrochemical behavior of TiN/Al in the sulfate solution is quite different from that in the chloride solution. Figure 19 shows potentiodynamic scans for TiN/glass, TiN/Al (1100), TiN/Cu, and bulk Cu in oxygen saturated 5 percent Na_2SO_4, pH=3.0. A polarization curve for bulk Al is not shown in the figure (it is very similar to that of TiN/Al, but at a much lower potential, starting from about -600 mV versus SCE). Note the very low current for TiN/Al. In this solution, 1100 Al is passive, hence there is no rapid corrosion of the Al substrate exposed to the sulfate solution due to pinholes. SEM examination of TiN/Al reveals virtually no change in the surface morphology after the corrosion test.

Unlike Al, Cu corrodes in the sulfate solution (Kim and Nobe 1971) hence the behavior of TiN/Cu in a sulfate solution is similar to that in a chloride solution. A TiN coating on Cu significantly reduces the exposed area, thus the anodic current relative to that of pure Cu. But the anodic current of TiN/Cu

* The free corrosion rate of Cu in oxygen saturated 3.5 percent NaCl, pH=6.0, was estimated as about 2 mil per year by a linear polarization technique and extrapolation of polarization curves to corrosion potential. This value is within the range of published value for static seawater (Fontana and Green).

is still very high compared to that of TiN/glass (Figure 19). Figure 20 shows cracking of the TiN coating caused by the spread of general corrosion of the Cu under the TiN coating. Note that a part of the cracked TiN around the original pinhole (marked by a small arrow) is raised, indicative of corrosion initiation at the pinhole. Because of this observation, it is possible that the pitting of TiN/Al in the chloride solution is also initiated at pinholes in spite of the lack of direct observation in this system.

Cu-Cr Alloy Coatings

Recently, Cu-Cr alloy systems have gained interest for use in the microelectronics industry because of a possible application of this alloy for stronger and better corrosion resistant conductive paths. A conventional fabricating technique of this alloy system had a very limited application because of the very small mutual solubilities between Cu and Cr in solid states. As shown in Figure 21, maximum solubility of Cr in Cu is only 0.65 weight percent at the eutectic temperature (1969.2 °F [1076.2 °C]) and virtually no Cu dissolves in Cr at all temperatures (ASM 1973). Current interest is to increase the solubility of Cr in Cu to obtain materials that may possess unique properties due to a metastable state. Several investigators (Shin et al. 1983; Kim and Yee 1985; Dirk and van der Broek; April 1985) have used physical vapor deposition techniques to produce metastable Cu-Cr alloys that contain much more Cr in Cu solid solution than that predicted by the phase diagram.

A series of Cu-Cr alloys fabricated at the ion-plating facility at USACERL were studied in terms of phase analysis and electrochemical behavior. Substrates were glass and CDA 110 Cu. Coating compositions were determined by wavelength-dispersive x-ray analysis. Pure Cu and Cr foils were used as reference standards and matrix corrections were continuously made during the analysis.

XRD results show that Cu-Cr alloys containing up to about 25 atomic percent CR consist of single phase FCC structure. The alloys containing more than 60 atomic percent Cr are single-phase BCC structure, and the alloys containing 25 to 60 atomic percent Cr have a dual-phase structure. Electrical resistivities of Cu-rich alloys, measured by a four-point probe technique, range from 6 μΩ-cm for pure Cu coating to about 30 μΩ-cm for 20 atomic percent Cr, which is substantially lower than that of TiN coating. Figure 22 shows a typical columnar structure of as-deposited Cu-10 atomic percent Cr [hereafter, CuCr(10)] coating on a glass substrate.

Anodic and cathodic potentiodynamic polarization scans for a series of Cu-Cr coatings on glass substrates in oxygen saturated 5 percent Na_2SO_4, pH=6.0, are shown in Figure 23 [polarization curve 1 for pure Cu coating, curve 2 for CuCr(10), curve 3 for CuCr(19), curve 4 for CuCr(40), and curve 5 for Cu-Cr(85)]. Note that Curves 1, 2, and 3 are from FCC structure, curve 4 from dual-phase structure, and curve 5 from BCC structure. The similarity of curves 2 and 3 to curve 1 and large anodic currents in these scans indicate that Cu-Cr alloy containing up to 19 atomic percent Cr behaves much like pure Cu. It does not appear from anodic scans that Cu-rich Cu-Cr coatings form a protective film. The free corrosion rates of these alloys were estimated as a few mils per year at pH=6.0, which is unacceptable. Hence, the desired result of alloying Cu with Cr to improve the corrosion resistance of Cu has not been achieved. A substantial decrease in the anodic current is observed only in the Cr-rich alloy (curve 5), but a Cr-rich alloy is not of interest for the present application.

Even though the performance of Cu-Cr coatings is not satisfactory, the electrochemical behavior of the coatings was studied in more detail to determine why a passive Cr film did not form on Cu-Cr coatings.

Three sets of Cu-rich Cu-Cr coatings were potentiostatically polarized at +25 mV versus SCE in oxygen saturated 5 percent Na_2SO_4, pH=6.0. The results are given in Figure 24 (A for current density

and B for coulombs). Polarization curve 1 is from pure Cu coating, curve 2 from CuCr(10), and curve 3 from CuCr(19). Note that the anodic current of pure Cu (2.2 milliamps per square centimeter [mA/cm_2] is reduced to about 0.5 mA/cm^2 with 19 atomic percent of Cr alloying. The tests in deaerated solutions show the same result as in oxygen saturated solutions. Figure 25 shows SEM micrographs of CuCr(10) after polarization to 0.48 C/cm^2 in an oxygen saturated solution. For the sake of direct comparison, SEM micrographs of as-deposited CuCr(10), Figure 22, are included on the left side of the figure. Note that the surface morphology of the corrosion tested sample is entirely different from that of the as-deposited sample. Among the morphological changes, formation of new crystals and fine pores in the tested sample deserve special attention. In a cross sectional view, the general film morphology, including the coating thickness, appears to be unchanged but the tested sample reveals a sponge-like structure while the as-deposited sample shows a dense structure. The possible explanation for these structural changes is that one element, possibly Cu, preferentially dissolves, leaving behind highly porous films (sponge-like structure) and corrosion products are deposited on the original film surface.

An Auger electron depth profile for the tested sample is shown in Figure 26. The sputtering rate is approximately 30 Å/min. Note the sharp change in Cu and Cr concentrations at about 1200 Å depth (42 minutes of sputtering time) indicating that the coating consists of two layers. In the first layer, Cu concentration increases with depth while the Cr concentration remains constant. In the second layer, both Cu and Cr concentrations are unchanged with depth. During the corrosion tests, if one element preferentially dissolves, or both elements dissolve at different rates, then the resulting concentration profiles will show gradual changes but no sharp change. The presence of a sharp change may indicate that the first layer is formed by redeposition of dissolved Cu and Cr on top of the original surface of the as-deposited sample. Considering the sensitivity factors of Cu and Cr Auger electrons, Cr concentration in the second layer is approximated as about 25 atomic percent, which is substantially larger than the original concentration in the 10 atomic percent as-deposited sample. This implies preferential dissolution of Cu, leaving behind a porous and Cr-enriched coating. However, some Cr dissolution cannot be ruled out because of the presence of Cr in the first layer. Gradual concentration profiles in the first layer indicate that the first layer consists of oxides (Cu_2O and Cr_2O_3) and elemental Cu and Cr; relative amounts of oxides decrease with increasing depth. This explanation is consistent with the SEM observation in Figure 25 but it is not conclusive and requires a more organized study to understand dissolution and redeposition kinetics in Cu-Cr coatings.

4 CONCLUSIONS

This research suggests that TiN coating is a suitable candidate for EMI shield application but Cu-Cr alloy coatings are not. However, the inherent problem of "pinholes" presents a serious obstacle to the use of TiN coating for corrosion protection of underlying metallic substrates over a long period of time. The following summarizes the results obtained throughout the course of this work.

TiN coatings fabricated at USACERL are essentially stoichiometric but the color is "brownish yellow" instead of the characteristic "gold" color of TiN as observed in commercial TiN, which is also stoichiometric. Both TiN coatings deposited on glass show passive behavior. A higher anodic current of the USACERL TiN (a few microamperes per square centimeter) than that of commercial TiN (about 0.1 $\mu A/cm^2$) is attributed to the presence of elemental Ti in the USACERL TiN, possibly located at the interface between the TiN coating and the glass substrate. A small amount of TiO_2 may be present throughout the coating thickness for the commercial TiN, but it is detected only at the very surface layer in the USACERL TiN. Short time polarization tests in a chloride solution cause the amount of TiO_2 at the surface of USACERL TiN to increase, which could increase contact resistance after a long service.

TiN coating on metallic substrates creates bielectrodes due to pinholes in the coatings. The pinholes do not cause any problem for TiN/Al in a sulfate solution, because Al itself is passive in a sulfate solution. However, a bielectrode nature of TiN/Al enhances pit growth of Al in a chloride solution, resulting in cracking and spalling of the TiN coating. The pits are apparently nucleated at the Al exposed by pinholes. Pitting of TiN/Al will seriously undermine the coating integrity and shielding effectiveness. TiN coating on Cu exhibits the same problem with pinholes but the anodic current of Cu is greatly reduced, because of a low corrosion rate and general corrosion of Cu in NaCl solutions. Hence, TiN/Cu does not cause as serious a problem as TiN/Al in chloride solution.

Metastable Cu-rich Cu-Cr alloy coatings behave much like copper, which shows a high anodic current and does not become passive. Reduction of the anodic current with 19 atomic percent Cr alloying in Cu is only nominal, hence the desired result of alloying with Cr to substantially improve the corrosion resistance of Cu was not achieved. The free corrosion rates of these alloy coatings are a few mils per year, which is unacceptable for thin film coating applications. Auger depth profiles and SEM examination of the tested sample indicate more active (or preferential) dissolution of Cu than Cr, causing a morphological change from an as-deposited dense structure to sponge-like structure.

REFERENCES

American Society for Metals (ASM) Handbook, 8th Edition, Vol. 8 (1973), p 290.

de De Micheli, S.M., "Electrochemical Study of Pitting Corrosion of Aluminum in Chloride Solutions," *Corrosion Science,* Vol 18 (1978), pp 605-616.

Dirk, A.G. and J.J. van der Broek, Paper presented at the 12th International Conference on Metallurgical Coatings, Los Angeles, April 1985.

Engineer Pamphlet (EP) 1110-3-2, *Electromagnetic Pulse (EMP) and TEMPEST Protection for Facilities* (Headquarters, U.S. Army Corps of Engineers, 31 December 1990).

Fontana, M.G., and N.D. Green, *Corrosion Engineering* (McGraw Hill, 1986).

Hintermann, H.E., "Tribological and Protective Coatings by Chemical Vapor Deposition," *Thin Solid Films*, Vol 84 (1981), pp 215-243.

Jamal, T., R. Nimmagadda, and R.F. Bunshah, "Friction and Adhesive Wear of Titanium Carbide and Titanium Nitride Overlay Coatings," *Thin Solid Films*, Vol 73 (1980), pp 245-254.

Kim, C.P., and K. Nobe, "Polarization of Copper in Acidic and Alkaline Solutions," *Corrosion,* Vol 27 (1971), pp 382-385.

Kim, J., and D.S. Yee, "Structures of Co-Evaporated Copper Alloys," *Thin Solid Films*, Vol 128 (1985), pp 67-68.

Meletis, E.I., W.B. Carter, and R.F. Hochman, "Corrosion Behavior of TiN Thin Films," Proceedings of the 17th Annual Technical Meeting of the International Metallographic Society, 15-18 July 1984, *Microstructural Science*, Vol 13 (1984), pp 417-432.

Rais, A.B F. Dalard, and J.C. Sohn, "Aluminum Pit Propagation in Acidic Media," *Corrosion Science*, Vol 25 (1985), pp 1035-1046.

Ramalingan, S., and W.O. Winer, "Reactively Sputtered TiN Coatings for Tribological Applications," *Thin Solid Films*, Vol 73 (1980), pp 267-274.

Robinson, K.S. and P.M.A. Sherwood, "X-ray Photoelectron Spectroscopic Studies of the Surface of Sputter Ion Plated Films," *Surface an Interface Analysis,* Vol 6 (1984), pp 261-266.

Shin, S.M., et al., "Growth of Metastable Cu (1-x) and Cr (x) Solid Solutions by Ion Mixing During Bias Sputter Deposition," *Applied Physical Letters*, Vol 43 (1983), pp 249-251.

Technical Manual (TM) 5-855-5, *Nuclear Electromagnetic Pulse (NEMP) Protection* (HQ, Department of the Army, February 1974).

Wittmer, M., "Properties and Microelectronic Applications of Thin Films of Refractory Metal Nitrides," *Journal Vacuum Science Technology*, Vol A3 (1985), pp 1797-1803.

Zeger, B., M. Kornman, and J. Aniquet, *Thin Solid Films*, Vol 45 (1977), p 577.

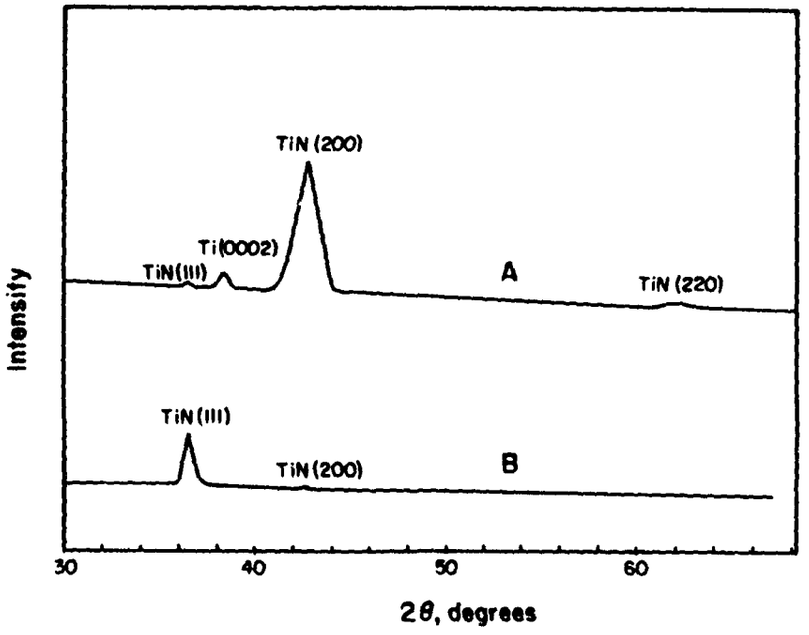

Figure 1. **X-ray Diffraction Spectra of As-deposited TiN Coatings.** (A, USACERL TiN and B, commercial TiN.)

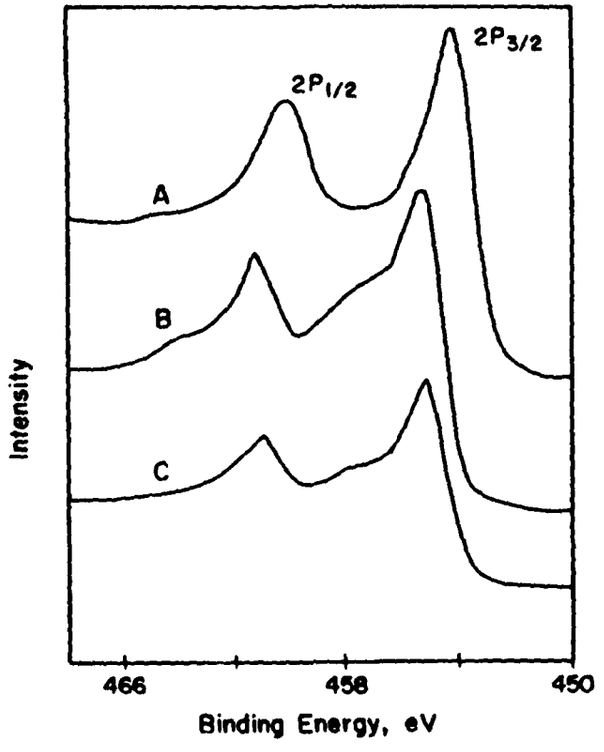

Figure 2. **Ti 2p X-ray Photoelectron Spectra of Commercial TiN, USACERL TiN, and Pure Ti After Removal of 10-20 Å of the Surface Layer.** (A, Ti; B, as-deposited commercial TiN; and C, as-deposited USACERL TiN.)

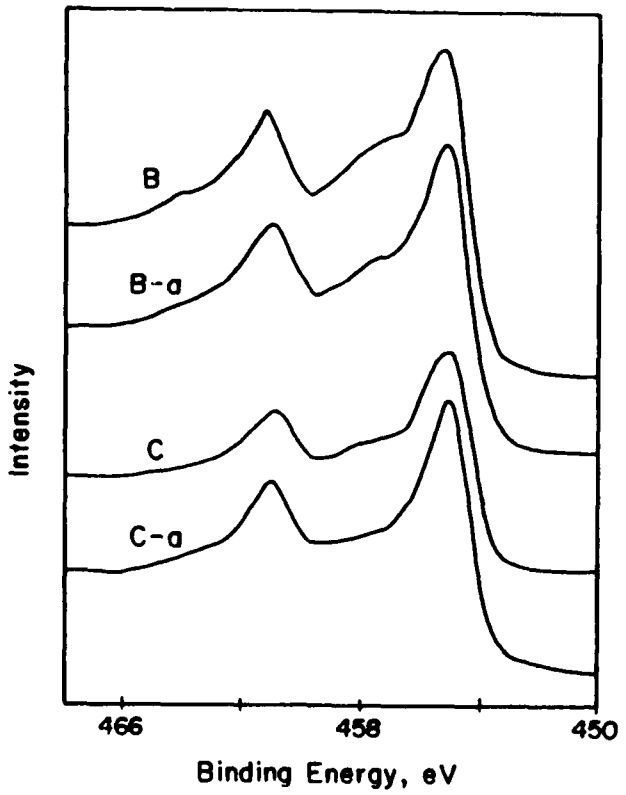

Figure 3. Ti 2p X-ray Photoelectron Spectra of TiN Coatings After Removal of About 100 Å of the Surface Layer. (Spectrum B and C are the same as in Figure 2, and Spectrum B-a and C-a are obtained after about 100 Å surface layer removal.)

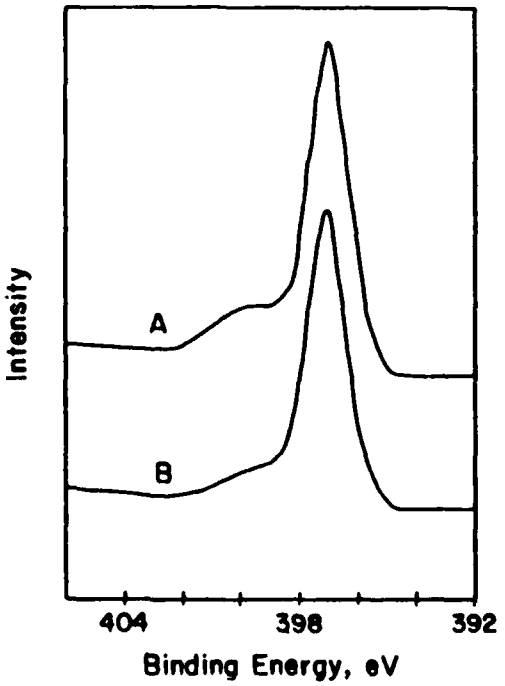

Figure 4. Nitrogen 1s XPS Spectra From TiN Coatings After Removal of About 100 Å of the Surface Layer. (A, commercial TiN and B, USACERL TiN.)

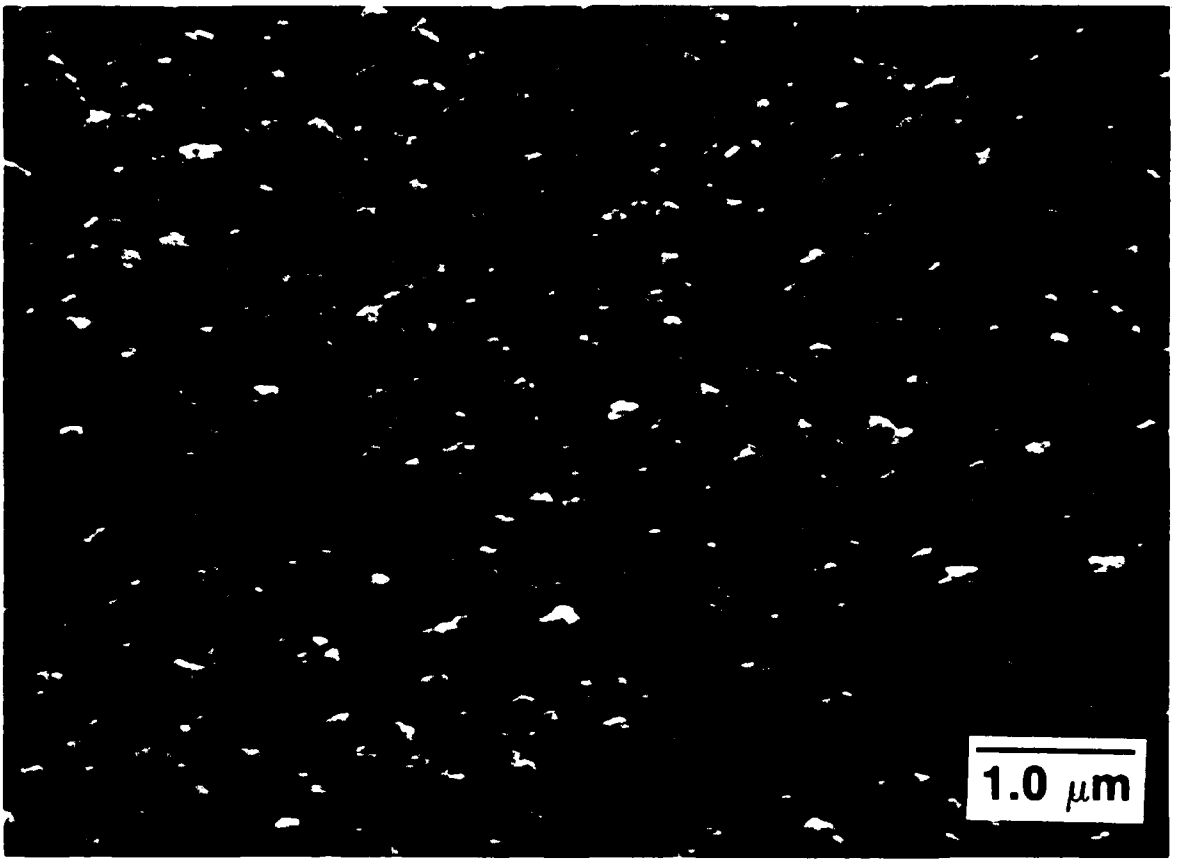

Figure 5. SEM Micrograph of As-deposited USACERL TiN on an Al Substrate. (7000X.)

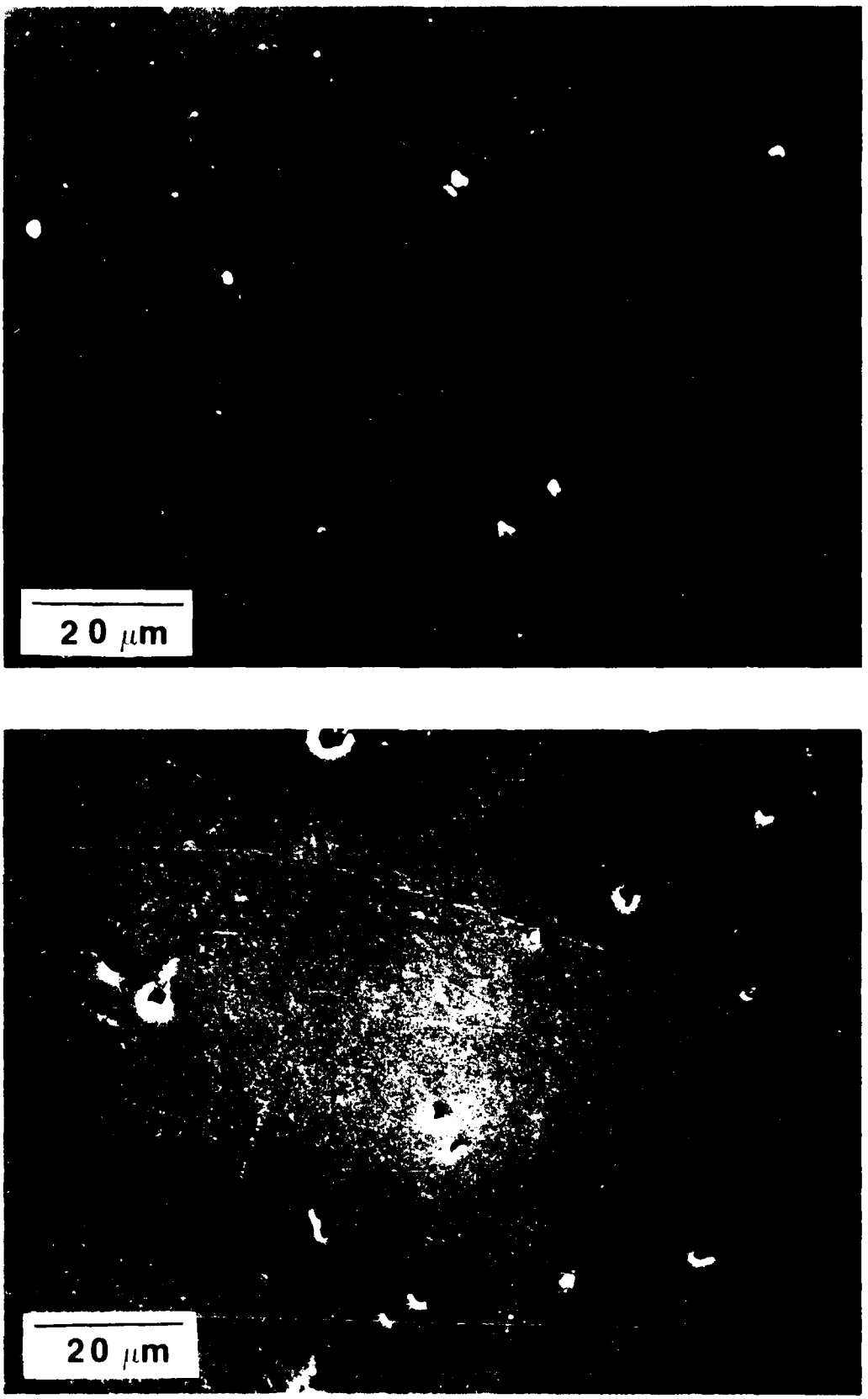

Figure 6. SEM Micrographs of As-deposited USACERL TiN on a Glass Substrate. (450X, A on glass and B on Al.)

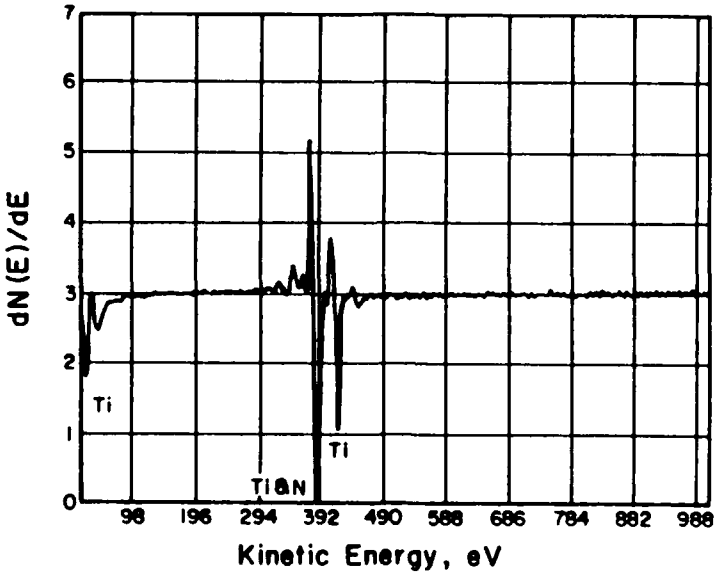

Figure 7. Auger Electron Spectra of As-deposited USACERL TiN After Removal of About 50 Å of the Surface Layer.

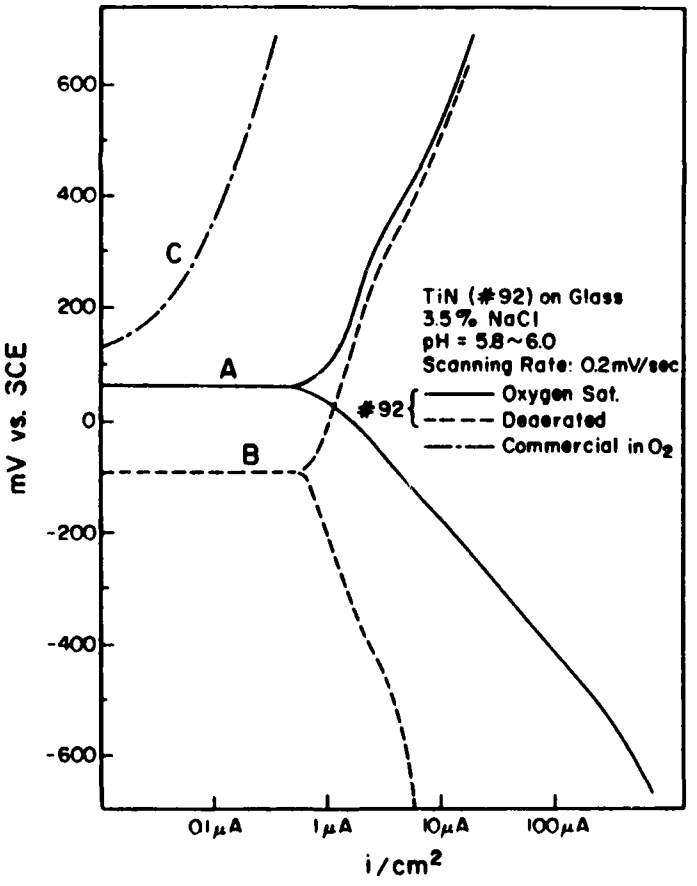

Figure 8. Potentiodynamic Anodic and Cathodic Scans of TiN/Glass in 3.5% NaCl, pH=6.0. (A, USACERL TiN in oxygen-saturated solution; B, USACERL TiN in deaerated solution; C, commercial TiN in oxygen-saturated solution.)

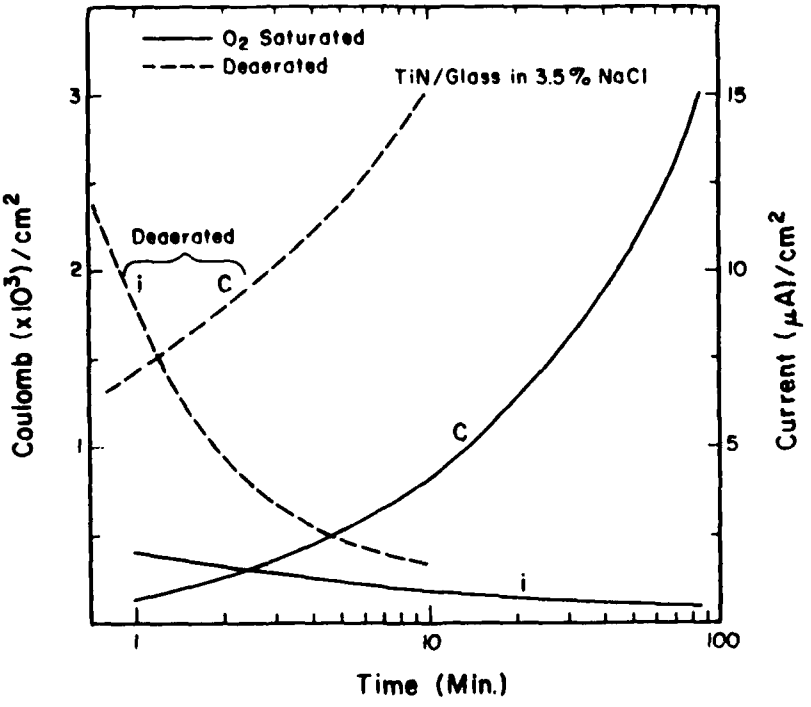

Figure 9. Potentiostatic Polarization Data of USACERL TiN/Glass in 3.5% NaCl, pH=6.0, at +300 mV vs SCE. (Dotted lines are for current density and coulombs in deaerated solution; solid lines in oxygen saturated solution.)

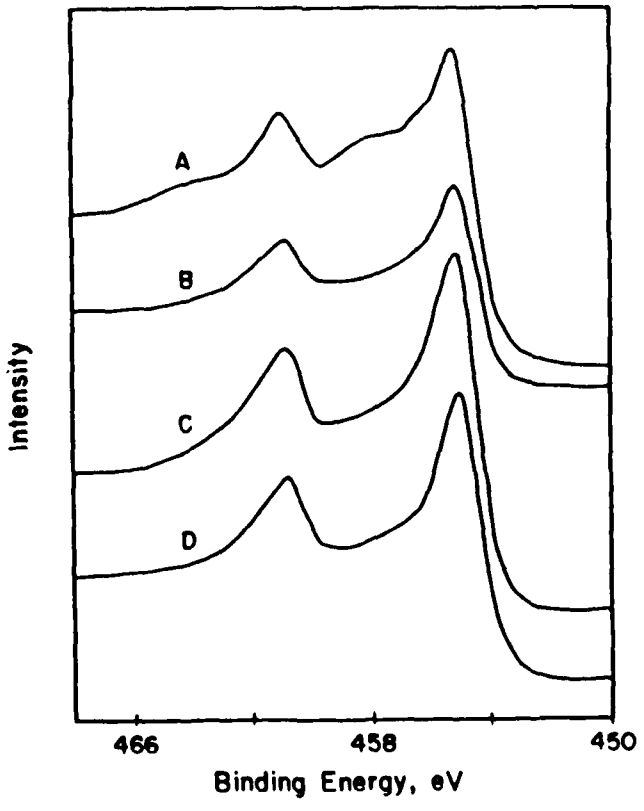

Figure 10. Ti 2p XPS Spectra of TiN After Potentiostatic Polarization Tests to 0.003 C at +300 mV vs. SCE in 3.5% NaCl, pH=6.0. (A and B in oxygen saturated solution, after removing about 10 and 100 Å of the surface layer. C and D in deaerated solution after removing about 10 and 100 Å of the surface layer.)

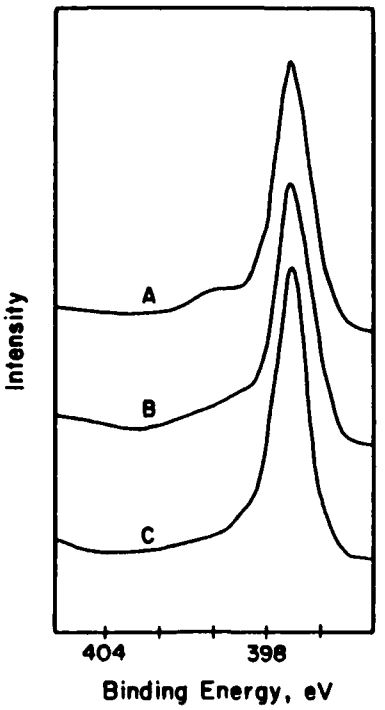

Figure 11. Nitrogen 1s XPS Spectra of TiN After Removal of About 10 Å of the Surface Layer After Potentiostatic Polarization Tests to 0.003 C in 3.5% NaCl, pH=6.0. (A, as-deposited; B, after test in oxygen-saturated solution; and C, in deaerated solution.)

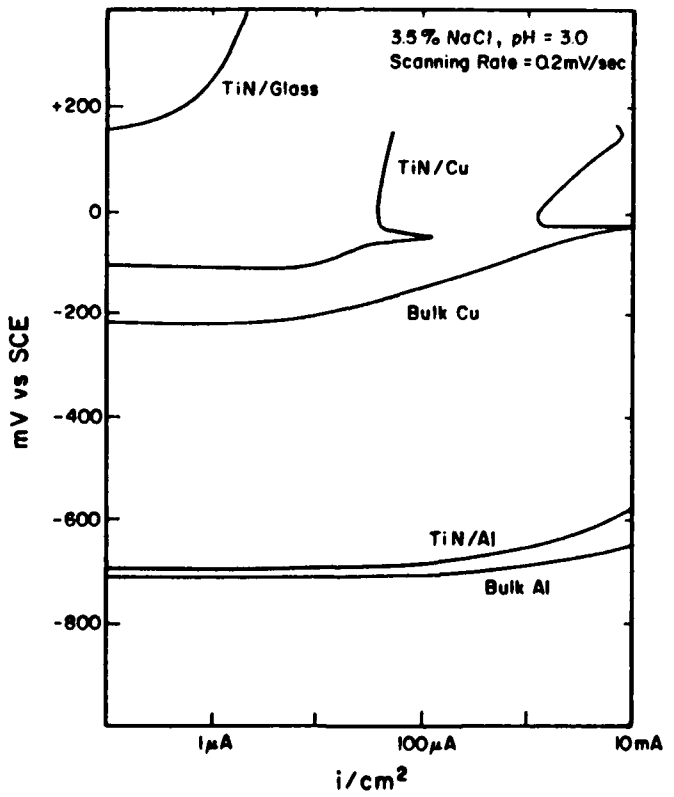

Figure 12. Potentiodynamic Polarization Scans in Oxygen-saturated 3.5% NaCl, pH=3, for TiN Coatings on Glass, Cu, and Al Substrates, and for Bulk Cu and Al Substrates.

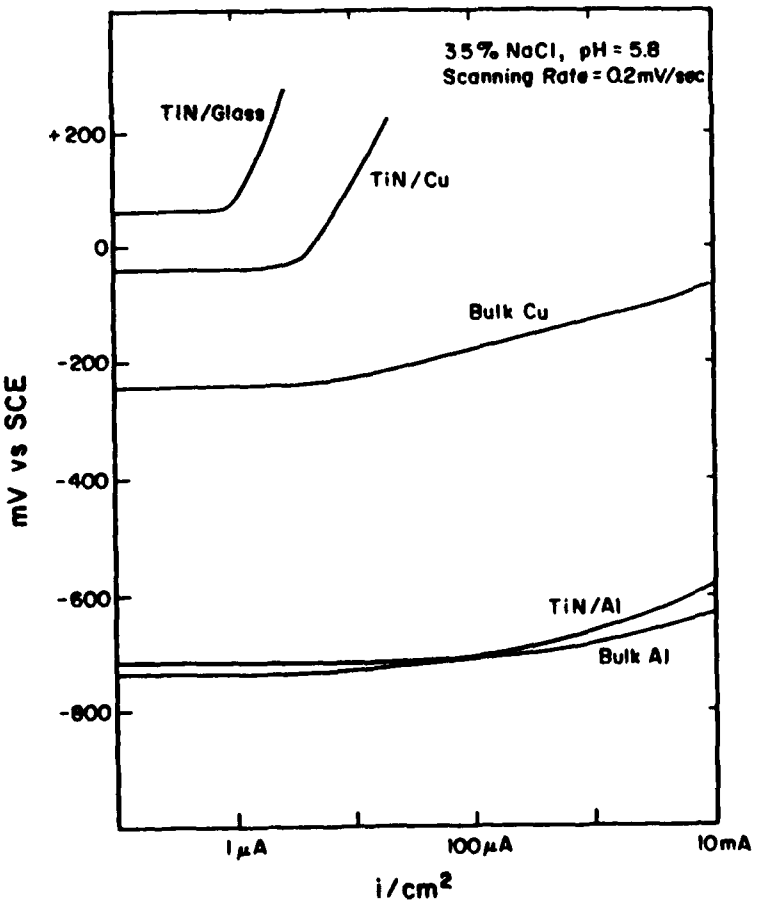

Figure 13. Potentiodynamic Polarization Scans in Oxygen-saturated 3.5% NaCl, pH=6.0.

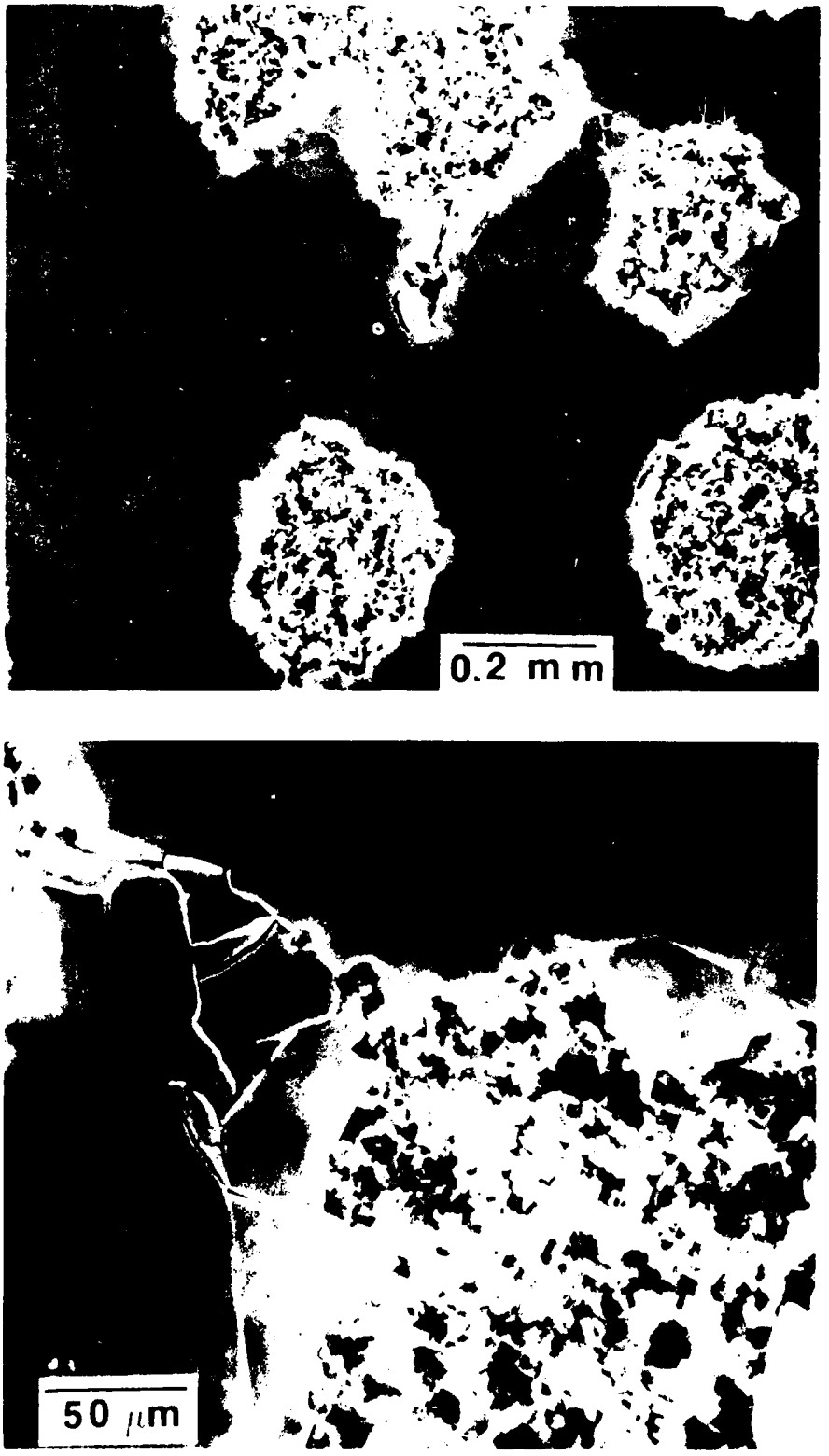

Figure 14. SEM Micrographs of TiN/Al Surface After Potentiodynamic Polarization Test in Oxygen-saturated 3.5% NaCl, pH=6.0.

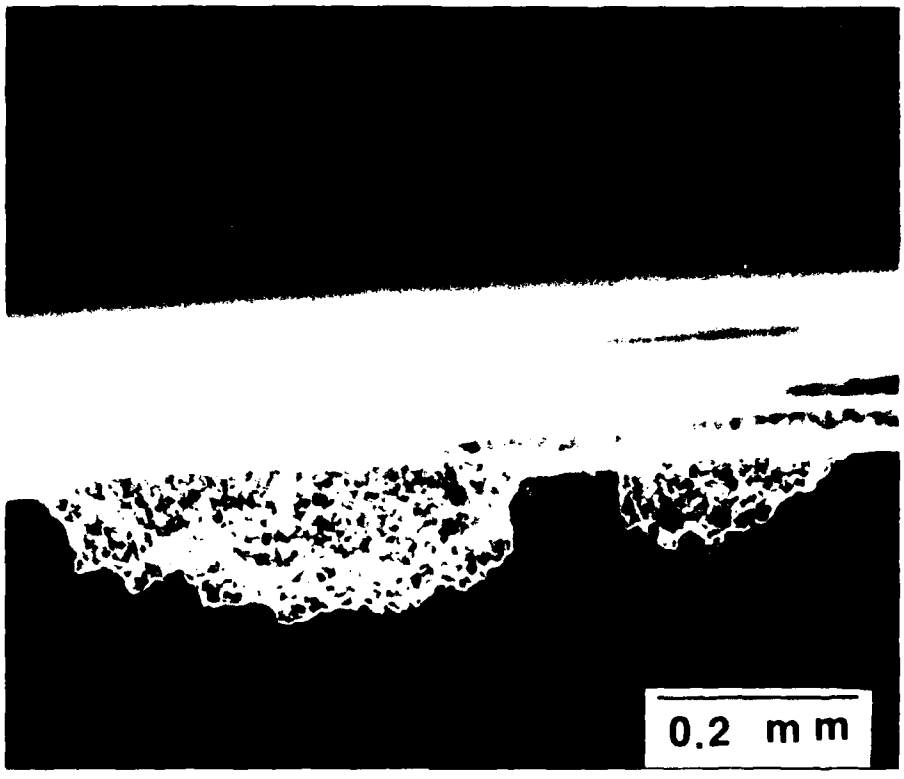

Figure 15. SEM Cross Section Micrographs of TiN/Al Surface After Potentiodynamic Polarization Test in Oxygen-saturated 3.5% NaCl, pH=6.0.

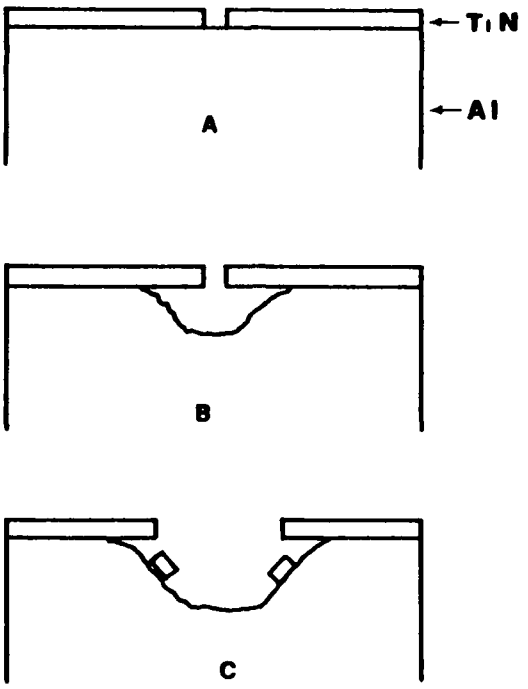

Figure 16. Schematic Diagram Showing Pit Initiation and Propagation, and TiN Coating Cracking for TiN/Al in Chlroide Solution.

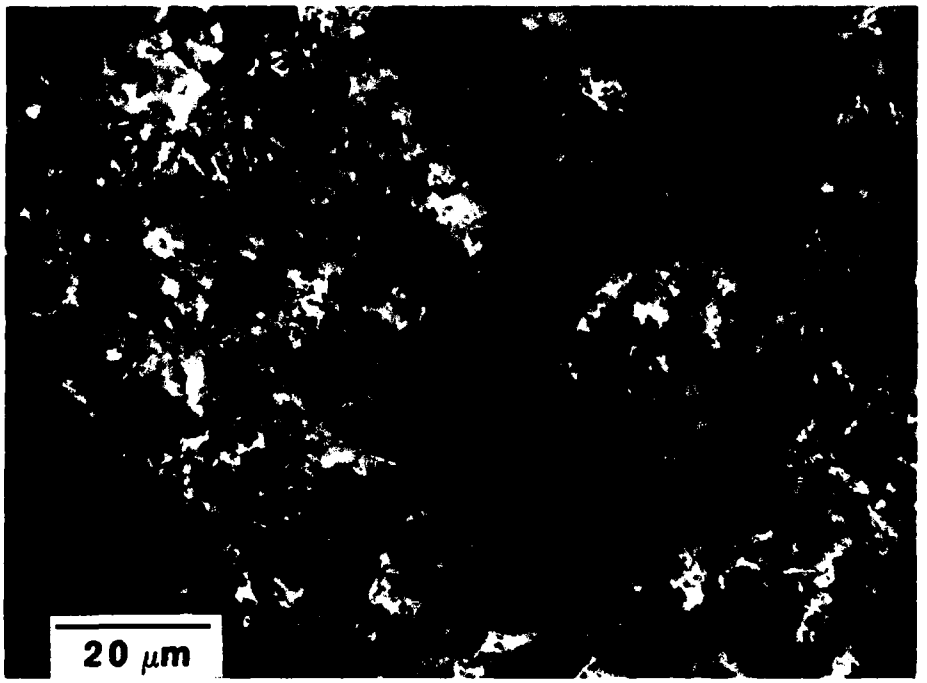

Figure 17. SEM Micrograph for Surface Morphology of Al After Anodic Polarization in Oxygen-saturated 3.5% NaCl, pH=6.0.

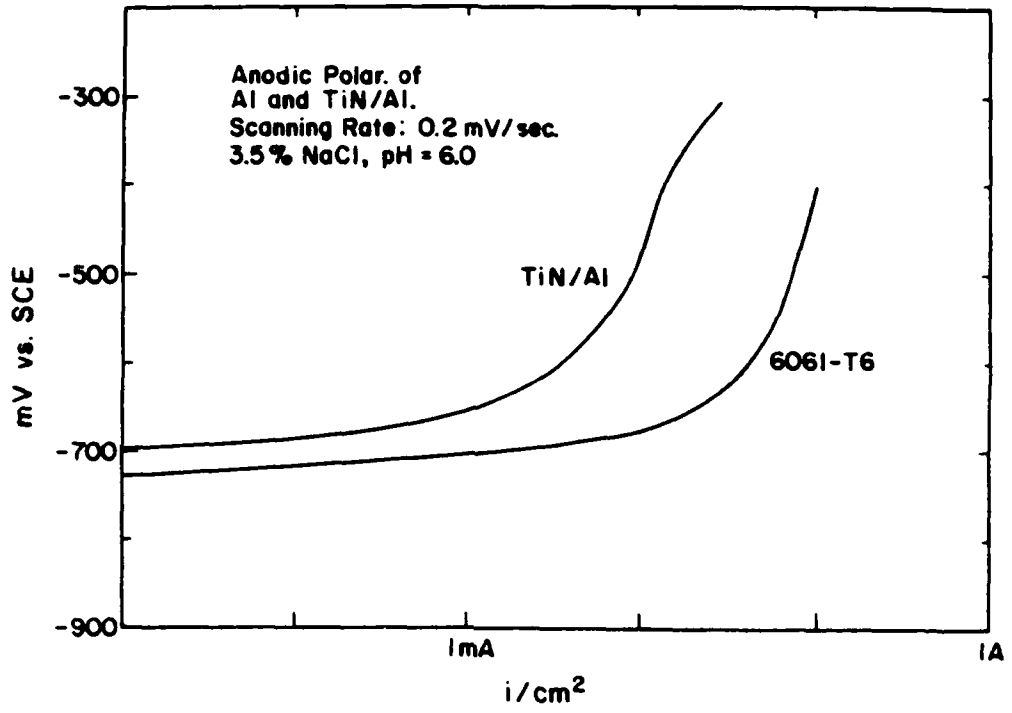

Figure 18. Potentiodynamic Polarization Scans for 6061-T6 Al and TiN/6061-T6 in Oxygen-saturated 3.5% NaCl, pH=6.0.

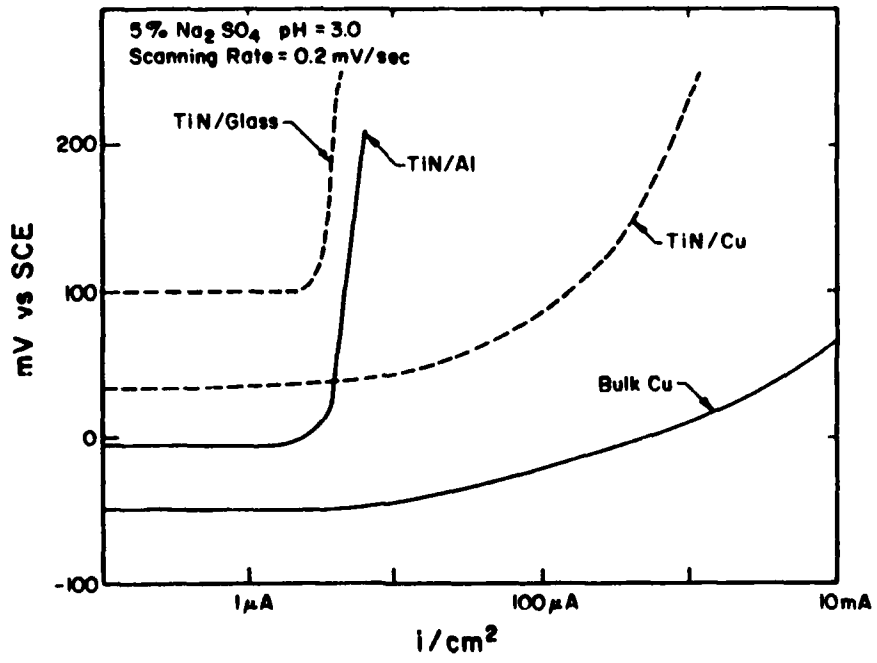

Figure 19. Potentiodynamic Polarization Scans in Oxygen-saturated 5% Na_2SO_4, pH=3 for TiN on Glass, Cu, and Al, and for Bulk Cu.

Figure 20. SEM Micrograph of TiN on Cu After Anodic Polarization Test in Oxygen-saturated 5% Na_2SO_4, pH=6.0.

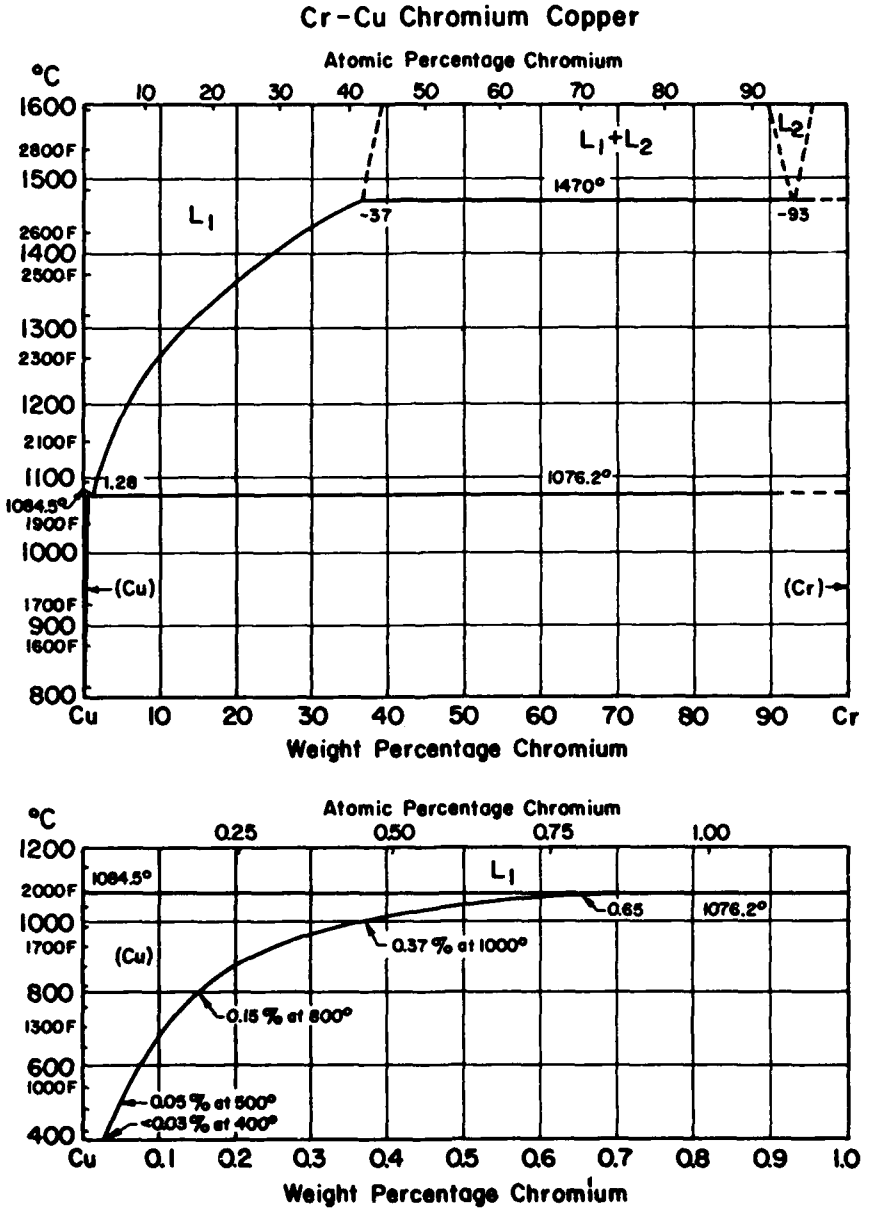

Figure 21. Equilibrium Cu-Cr Binary Phase Diagram.

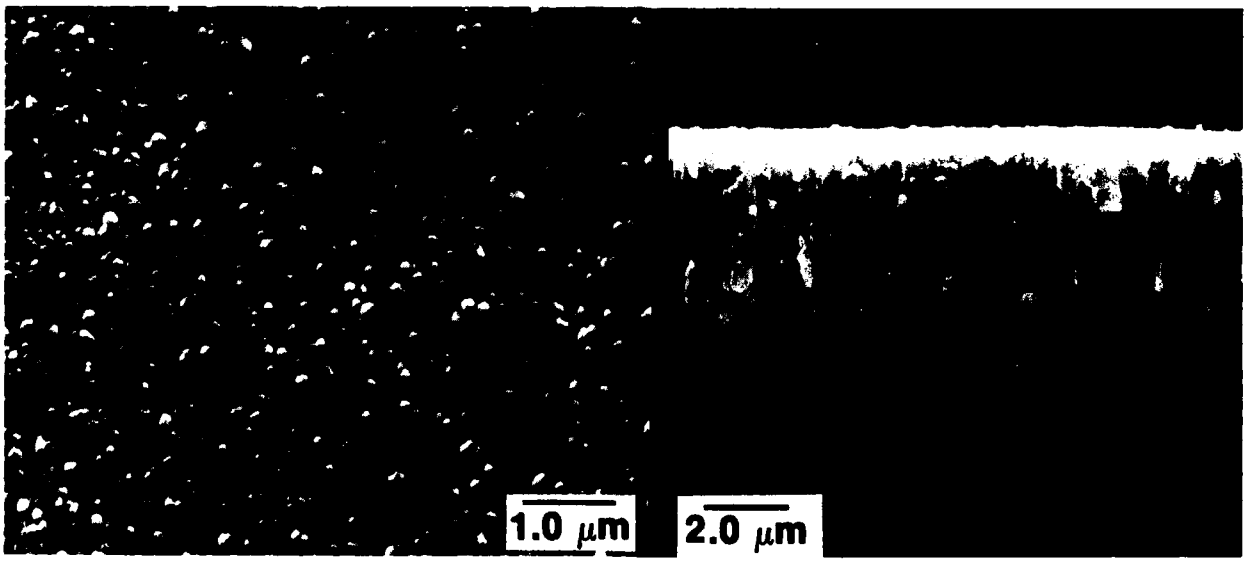

Figure 22. SEM Micrographs of As-deposited CuCr(10) on Glass.

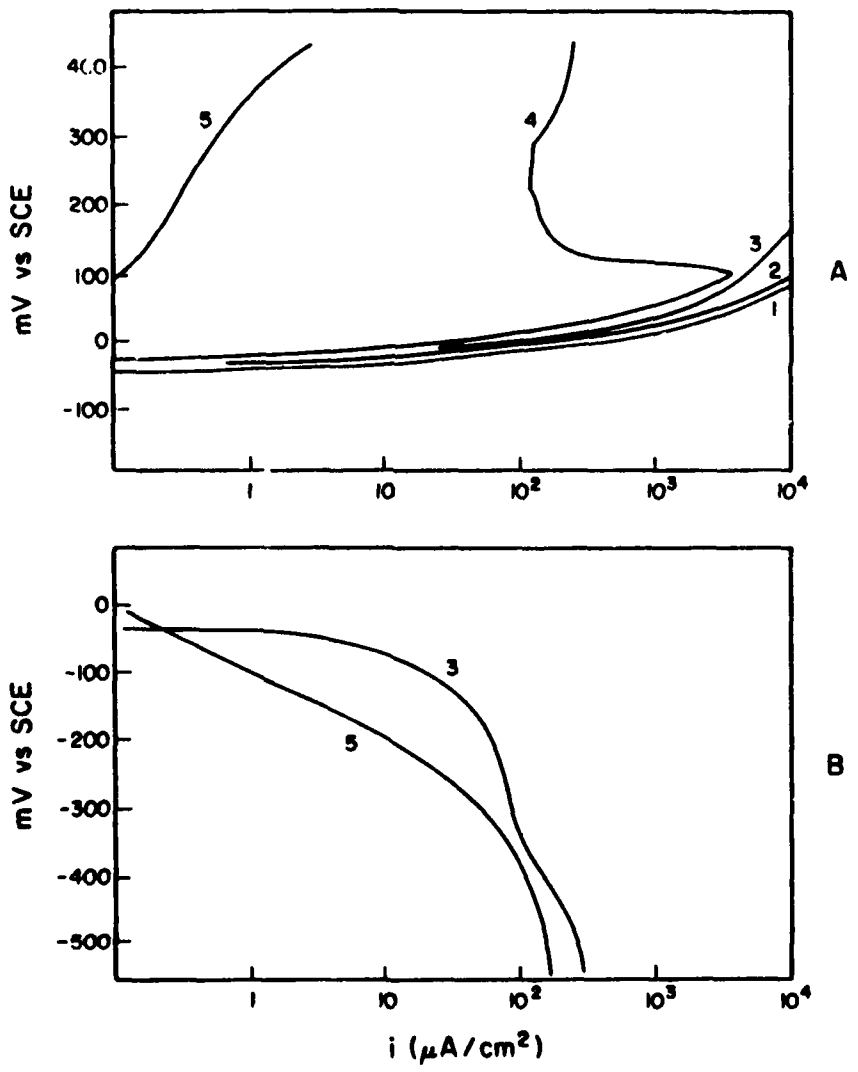

Figure 23. Anodic and Cathodic Polarization Scans for Cu-Cr Alloy Coatings in Oxygen-saturated 5% Na_2SO_4, pH=6.0. [A, anodic; B, cathodic; 1, pure Cu; 2, CuCr(10); 3, CuCr(19); 4, CuCr(40); and 5,CuCr(85).]

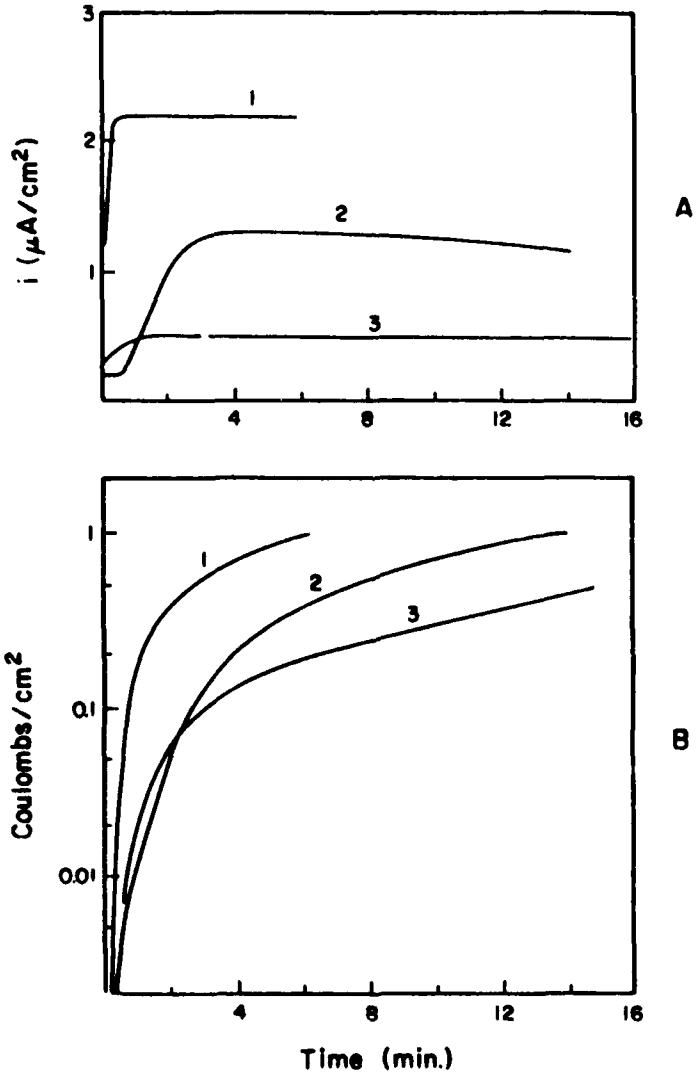

Figure 24. Potentiostatic Scans of Cu-Cr Coatings Showing Current Density Change and Coulombs Change With Time at +25 mV vs SCE in Oxygen-saturated 5% Na_2SO_4, pH=6.0. [A, density change; B, Coulombs; 1, pure Cu; 2, CuCr(10); 3, CuCr(19).]

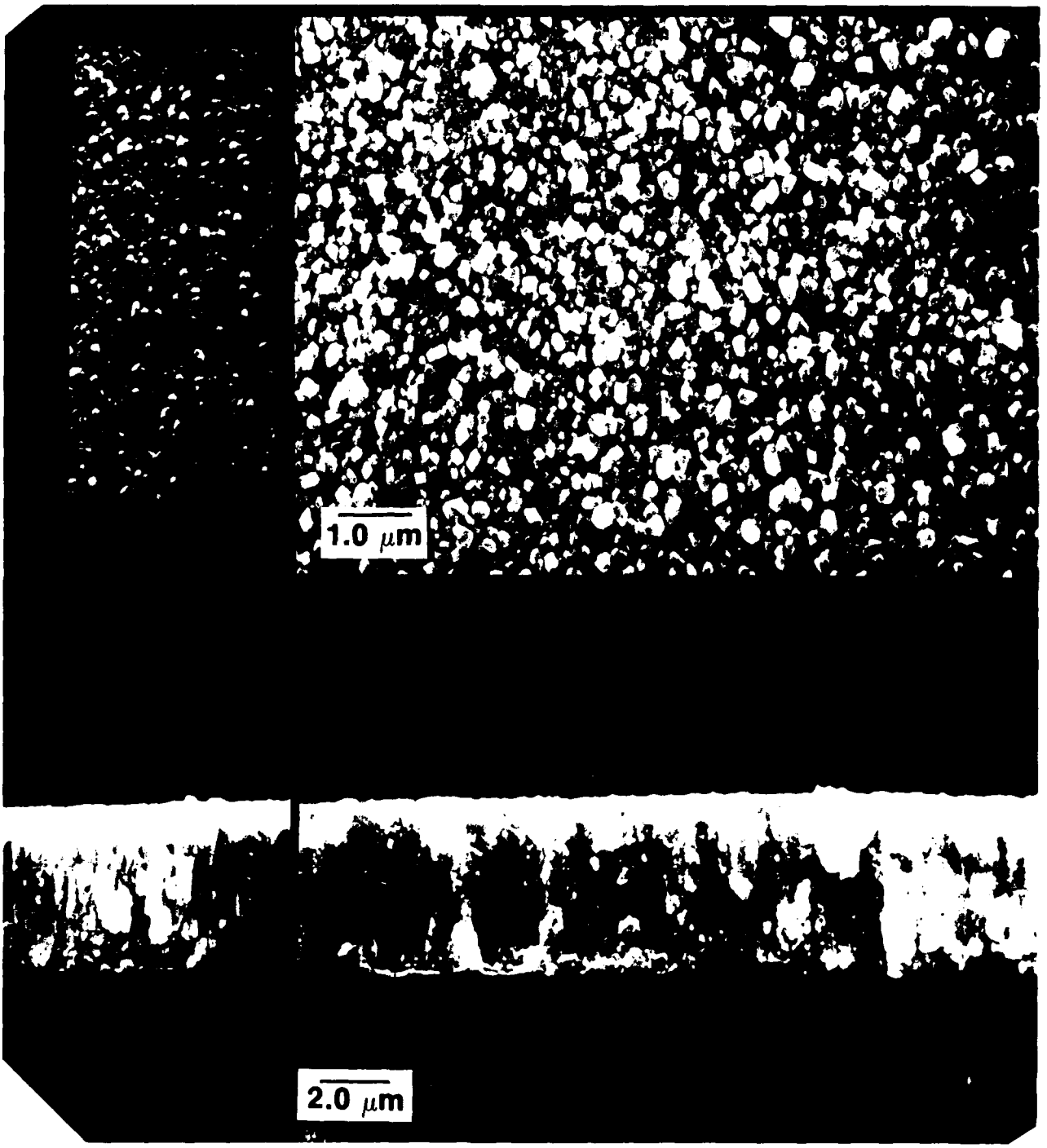

Figure 25. SEM Micrographs of CuCr(10) After Potentiostatic Test to 0.48 C/CM^2 in Oxygen-saturated Na_2SO_4 at +25 mV vs SCE. [For direct comparison, SEM micrographs of as-deposited CuCr(10) are included (smaller ones).]

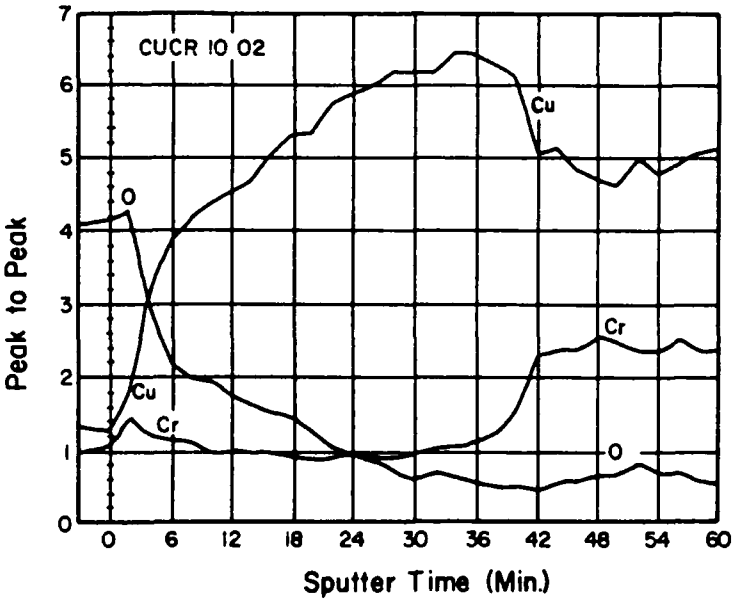

Figure 26. AES Depth Profile of CuCr(10) After Potentiostatic Test.

DISTRIBUTION

US Army Engineer District
New York 10278
ATTN: Chief, Design Br
Pittsburgh 15222
ATTN: Chief, Engr Div
Philadelphia 19106
ATTN: Chief, NAPEN-D
Baltimore 21203
ATTN: Chief, Engr Div
Norfolk 23510
ATTN: Chief, NAOEN-M
ATTN: Chief, NAOEN-D
Huntington 25701
ATTN: Chief, Design Br
Wilmington 28402
ATTN: Structures Sec
ATTN: Chief, SAWEN-D
Charleston 29402
ATTN: Chief, Engr Div
Savannah 31402
ATTN: Chief, SASAS-L
Jacksonville 32232
ATTN: Constr Branch
ATTN: Dgn Br, Structures Sec
Mobile 36628
ATTN: Chief, SAMEN-D
ATTN: Chief, SAMEN-C
Nashville 37202
ATTN: Chief, ORNED-D
Memphis 38103
ATTN: Chief, CELMM-ED-D
ATTN: Chief, CELMM-ED-M
Vicksburg 39180
ATTN: Chief, Engr Div
Louisville 40201
ATTN: Chief, Engr Div
Detroit 48231
ATTN: Chief, NCEED-T
St. Paul 55101
ATTN: Chief, ED-D
Chicago 60606
ATTN: Chief, NCCED-DS
Rock Island 61204
ATTN: Chief, Engr Div
ATTN: Chief, NCRED-D
St. Louis 63101
ATTN: Chief, ED-D
Kansas City 64106
ATTN: Chief, Engr Div
Omaha 68102
ATTN: Chief, Engr Div
New Orleans 70160
ATTN: Chief, LMNED-DG
Little Rock 72203
ATTN: Chief, Engr Div
Tulsa 74121
ATTN: SWTED
Fort Worth 76102
ATTN: Chief, SWFED-D
Galveston 77553
ATTN: Chief, SWGAS-L
ATTN: Chief, SWGED-DS
ATTN: Chief, SWGED-D
Albuquerque 87103
ATTN: Chief, Engr Div
Los Angeles 90053
ATTN: Chief, SPLED-D
San Francisco 94105
ATTN: Chief, Engr Div
Sacramento 95814
ATTN: Chief, SPKED-D
Far East 96301
ATTN: POFED-L
Portland 97208
ATTN: EN-DB-SA
ATTN: Chief, DB-3
Seattle 98124
ATTN: Chief, NPSCO
ATTN: Chief, NPSEN-DB-M
ATTN: Chief, NPSEN-DB-ST
ATTN: NPSEN-PL-WC
Walla Walla 99362
ATTN: Chief, Engr Div
Alaska 99506
ATTN: Chief, NPAEN-G-M

US Army Engineer Division
New England 02254
ATTN: Chief, NEDED-T
North Atlantic 10007
ATTN: Chief, NADEN-T
ATTN: Library
Middle East (Africa) 22601
ATTN: Library
South Atlantic 30335
ATTN: Chief, SADEN-TS
ATTN: Chief, SADEN-TE
Huntsville 35807
ATTN: Chief, HNDED-CS
ATTN: Chief, HNDED-SR
ATTN: Chief, HNDED-SY
Ohio River 45201
ATTN: Chief, Engr Div
North Central 60605
ATTN: Chief, Engr Div
Missouri River 68101
ATTN: Chief, MRDED-T
Southwestern 75242
ATTN: Chief, SWDED-TS
ATTN: Chief, SWDED-TM
South Pacific 94111
ATTN: Chief, SPDED
Pacific Ocean 96858
ATTN: Chief, Engr Div
ATTN: Chief, FM&S Branch
ATTN: Chief, PODED-D
North Pacific 97208
ATTN: Chief, Engr Div

7th US Army 09407
ATTN: AETTM-DTT-MG-EH

US Liaison Detachment 10007
ATTN: Library

Griffiss AFB 13440
ATTN: ADC/RBES

Bolling AFB 20332
ATTN: AF/LEEEU

Defense Nuclear Agency 20305
ATTN: DNA-RAEV (2)
ATTN: DNA-DDST
ATTN: DNA-STRA
ATTN: DNA-RAEE 22310

USA NATICK 01760
ATTN: STRNC-UE
ATTN: STRNC-US

Harry Diamond Labs 20783
ATTN: SLCHD-NW-ED
ATTN: SLCHD-NW-P
ATTN: SLCHD-NW-EC
ATTN: SLCHD-NW-EE

Naval Air Systems Command 20360
ATTN: Library

Ft. Lee 23801
ATTN: AMXMC-D (2)

Ft. Monmouth 07703
ATTN: DRSEL-LE-SS

ARRADCOM 07801
ATTN: DRDAR-LCA-OK

SHAPE 09055
ATTN: Infrastructure Br

Hanscom AFB, MA 01731
ATTN: HQ AFSC
ATTN: ESD/OCMS

Aberdeen Proving Ground 21010
ATTN: NGB-ARI-E

Ft. Belvoir, VA 22060
ATTN: Capitol Area Office
ATTN: Defense CEETA

Ft. Leonard Wood MO 65473
ATTN: Clarke Engr School Library

Ft. Monroe, VA 23651
ATTN: ATEN-FN (2)
ATTN: ATEN-FE-W
ATTN: ATEN-AD

FORSCOM 30330
ATTN: AFEN-CD

NAVFAC 22332
ATTN: Code 04

Naval Training Ctr 32813
ATTN: Library

CEWES 39180
ATTN: WESSV-Z

Ft. Leavenworth, KS 66027
ATTN: ATZLCA-SA

Little Rock AFB, AR 72099
ATTN: 314/DEEE

Port Hueneme 93043
ATTN: Morell Library

Tinker AFB, OK 73145
ATTN: 2854 ABG/DEEE

Kirtland AFB, NM 87117
ATTN: AFWL/NTE
ATTN: AFWL/CED

Tyndall AFB, FL 32403
ATTN: AFESC/PRT
ATTN: AFESC/RDCF

US Army Foreign Sci. & Tech Ctr
ATTN: Charlottesville 22901
ATTN: Far East Office 96328

HQ, Combined Field Army (ROK/US)
ATTN: CFAR-EN 96358

Wright-Patterson AFB, OH 45433
ATTN: ASD/ENAMA
ATTN: AFWAL/MLSE

Naval Civil Engr Lab 93041
ATTN: Library

Camp Humphreys 96721
ATTN: Engineer

Transportation Research Board 20418

Building Research Board 20418

Dept of Transportation 20590

Chief of Engineers
ATTN: CERD-L
ATTN: CEMP-EE
ATTN: CEHEC-IM-LP (2)
ATTN: CEHEC-IM-LH (2)

Defense Technical Info. Ctr. 22304
ATTN: DTIC-FAB (2)

USACPW 55060
ATTN: Library
ATTN: PREP
ATTN: CECC-R